

# Ultrasound Contrast Imaging - Improved Tissue Suppression in Amplitude Modulation

**Erlend Fagertun Hofstad**

Master of Science in Communication Technology

Submission date: June 2006

Supervisor: Tor Audun Ramstad, IET

Co-supervisor: Sigmund Frigstad, GE Vingmed Ultrasound  
Hans Torp, ISB



# Problem Description

Today pulse inversion is used by GE Vingmed Ultrasound AS to utilize the nonlinear properties of the bubbles in contrast based ultrasound imaging. Other techniques, including amplitude modulation, are considered. But there might be a problem using these techniques, as the transmitted pulses with different amplitude on the Vivid7 US scanner suffer from a lack of symmetry, which causes an insufficient suppression of linear signal from surrounding tissue. The task is to investigate this problem in detail. Furthermore should the candidate suggest, develop and test out new methods to improve CTR (Contrast-to-Tissue-Ratio), without affecting the CNR (Contrast-to-Noise-Ratio).

Assignment given: 16. January 2006  
Supervisor: Tor Audun Ramstad, IET



# Abstract

The ability to image myocardial perfusion is very important in order to detect coronary diseases. GE Vingmed Ultrasound uses contrast agent in combination with a pulse inversion (PI) technique to do the imaging. But this technique does not function sufficiently for all patients. Therefore have other techniques been tested out, including transmission of pulses with different amplitude (AM), to enhance the nonlinear signal from contrast bubbles. But a problem achieving sufficient cancellation of linear tissue signal is a feebleness of the method.

In this diploma work has an effort been put into enhancing the tissue suppression in amplitude modulation. First the source of the lack of suppression was searched for by measuring electrical and acoustical pulses. The further examination revealed a dissymmetry in between pulses of different amplitude. To reduce this error were several attempts to make a compensation filter performed, which finally resulted in a filter created of echo data acquired from a tissue mimicking phantom. The filter was furthermore tested out on a flow phantom to see how it affected the signal from tissue and contrast bubbles, compared to the former use of a constant instead of the filter. The comparison showed 1.5-3.2 dB increase in tissue suppression (TS). But unfortunately did the filtering process slightly reduce the contrast signal as well, which resulted in a smaller increase of Contrast-to-Tissue-Ratio (CTR) than TS; 1.0-2.8 dB.

During the work was the source of another problem concerning tissue suppression discovered. In earlier work by the author [12] the experimental results suffered from low TS around the transmitted frequency, which was found inexplicable at that time. This problem was revealed to be caused by reverberations from one pulse, interfering with the echoes from the next pulse. The solution suggested in this thesis is to transmit pulses in such a way that every pulse used to create an image has a relatively equal pulse in front. For instance, if a technique employs two pulses to create an image, and the first has half the amplitude and opposite polarity of the second. Then, to eliminate the reverberations must the first imaging pulse have a pulse in front which has half the amplitude and opposite polarity of the pulse in front of the second imaging pulse.

# Preface

This thesis is the final part of the MSc study at the Norwegian University of Science and Technology. The work has been carried out at the Department of Circulation and Medical Imaging. My supervisors have been Sigmund Frigstad at GE Vingmed Ultrasound AS and Professor Hans Torp at the Department of Circulation and Medical Imaging. I am grateful for all their help and assistance during the work. I would also like to offer Mona Opshal at the Department of Circulation and Medical Imaging my gratitude for help with data acquisition. And finally I thank all my fellow students at the department for a great social and working environment.

Erlend Fagertun Hofstad

# Contents

<b>1</b>	<b>Introduction</b>	<b>1</b>
<b>2</b>	<b>Theory</b>	<b>2</b>
2.1	Ultrasound Imaging . . . . .	2
2.1.1	Basic principle of Ultrasound Imaging . . . . .	2
2.1.2	IQ demodulation . . . . .	3
2.1.3	The Mechanical Index (MI) . . . . .	4
2.2	Image quality in ultrasound . . . . .	4
2.2.1	Spatial resolution . . . . .	4
2.2.2	Contrast resolution . . . . .	5
2.3	Ultrasound contrast imaging . . . . .	6
2.3.1	The contrast agent . . . . .	6
2.3.2	Scatters from contrast agent . . . . .	6
2.3.3	Non-linear propagation in tissue . . . . .	8
2.4	Detection techniques of ultrasound contrast bubbles . . . . .	9
2.4.1	Pulse inversion . . . . .	9
2.4.2	Amplitude modulation . . . . .	10
2.4.3	Combination of PI and AM . . . . .	12
<b>3</b>	<b>Measurements</b>	<b>13</b>
3.1	Electrical pulses . . . . .	13
3.2	Acoustical pulses . . . . .	13
3.3	Acquisition of phantom data . . . . .	14
3.3.1	Scanner settings . . . . .	15
3.3.2	Reverberation problem . . . . .	16
3.3.3	Acquisition . . . . .	16
3.3.4	Tissue phantom . . . . .	18
<b>4</b>	<b>Processing of IQ-data</b>	<b>19</b>
4.1	IQ-data . . . . .	19
4.2	Region of interest . . . . .	19
4.3	Validation of the constant AM factor . . . . .	19
4.4	The AM filter . . . . .	20
4.4.1	Filter from electrical pulses . . . . .	21
4.4.2	Filter from acoustical pulses . . . . .	21
4.4.3	Filter from tissue data . . . . .	21
4.4.4	Filter applied in AM . . . . .	23
4.4.5	Filter issues . . . . .	24
4.5	Quality measurement: CTR, CNR and TS . . . . .	25

<b>5</b>	<b>Results</b>	<b>28</b>
5.1	Transmitted pulses with different amplitude . . . . .	28
5.2	Suppression by AM . . . . .	29
5.3	Reverberations . . . . .	31
5.4	AM filters . . . . .	33
5.4.1	Filter from electrical and acoustical pulses . . . . .	33
5.4.2	Filter from tissue data . . . . .	34
<b>6</b>	<b>Discussion</b>	<b>43</b>
6.1	Choice of settings . . . . .	43
6.2	Transmitted pulses . . . . .	43
6.2.1	Two HV-power supplies . . . . .	43
6.3	Reverberation problem in AM . . . . .	44
6.4	Filter vs. constant in AM . . . . .	45
6.4.1	Filter from electrical and acoustical pulses . . . . .	45
6.4.2	Filter from tissue data . . . . .	45
6.5	Which modulation technique is best? . . . . .	47
6.6	Influence of pulse length . . . . .	47
<b>7</b>	<b>Suggested future work</b>	<b>49</b>
<b>8</b>	<b>Conclusion</b>	<b>50</b>
<b>A</b>	<b>Appendix</b>	<b>53</b>
A.1	Tissue Suppression . . . . .	53
A.2	Contrast-to-Tissue-Ratio . . . . .	54
A.3	Contrast-to-Noise-Ratio . . . . .	55



## List of Figures

1	<i>Ultrasound imaging system</i> . . . . .	2
2	<i>IQ demodulation</i> . . . . .	3
3	<i>Asymmetric oscillation of an ultrasound contrast bubble</i> . . . . .	7
4	<i>Non-linear propagation in tissue</i> . . . . .	9
5	<i>Pulse inversion</i> . . . . .	11
6	<i>Amplitude modulation</i> . . . . .	12
7	<i>Experimental setup</i> . . . . .	15
8	<i>Tissue and contrast areas used in the analysis</i> . . . . .	20
9	<i>Electrical pulses and filter frequency spectrum, 10 and 5 V</i> . . . . .	22
10	<i>Acoustical pulses and filter frequency spectrum, 10 and 5 V</i> . . . . .	23
11	<i>ROI from tissue phantom</i> . . . . .	24
12	<i>AM filter from tissue data. Length 150, no smoothing.</i> . . . . .	25
13	<i>AM filter from tissue data. Length 25, no smoothing.</i> . . . . .	26
14	<i>AM filter from tissue data. Length 25, smoothed.</i> . . . . .	27
15	<i>Electrical pulses</i> . . . . .	28
16	<i>Acoustical pulses</i> . . . . .	29
17	<i>Suppression of electrical pulses</i> . . . . .	30
18	<i>Suppression by AM of acoustical pulses</i> . . . . .	31
19	<i>Echo-data from the tissue phantom suppressed by AM</i> . . . . .	32
20	<i>Reverberations in amplitude modulation</i> . . . . .	33
21	<i>Frequency specter of a tissue area from the images in figure 20.</i> . . . . .	34
22	<i>Different filters used in AM</i> . . . . .	35
23	<i>Tissue suppressed by AM: constant, electrical and acoustical filter. 10/5V</i> .	36
24	<i>Filter from phantom data: AM, 2.5 periods, 5/3.79V, Optison.</i> . . . . .	37
25	<i>Grayscale images from 24.</i> . . . . .	37
26	<i>Filter from phantom data: AM, 2.5 periods, 7/5V, Optison.</i> . . . . .	38
27	<i>Grayscale images from 26.</i> . . . . .	38
28	<i>Filter from phantom data: AM, 2.5 periods, 10/6.84V, Optison.</i> . . . . .	39
29	<i>Grayscale images from 28.</i> . . . . .	39
30	<i>TS for 2.5 periods pulses.</i> . . . . .	40
31	<i>TS for 3.5 periods pulses.</i> . . . . .	40
32	<i>CTR for 2.5 periods pulses and Optison contrast agent.</i> . . . . .	41
33	<i>CNR for 2.5 periods pulses and Optison contrast agent.</i> . . . . .	41
34	<i>CTR for 2.5 periods pulses and Sonazoid contrast agent.</i> . . . . .	42
35	<i>CNR for 2.5 periods pulses and Sonazoid contrast agent.</i> . . . . .	42

## List of Tables

1	<i>Typical B/A values</i> . . . . .	8
2	<i>Equipment used meassuring electrical pulses</i> . . . . .	13
3	<i>Equipment used meassuring acoustical pulses</i> . . . . .	14
4	<i>Equipment used in the acquisition of flow phantom data</i> . . . . .	14
5	<i>Equipment used in the acquisition of tissue phantom data</i> . . . . .	18
6	<i>Tissue suppression after AM with different filters</i> . . . . .	35
7	<i>AM: Improved TS, CTR and CNR with AM filter</i> . . . . .	46
8	<i>AM: Tissue Suppression [dB]</i> . . . . .	53
9	<i>PIAM: Tissue Suppression [dB]</i> . . . . .	53
10	<i>PI: Tissue Suppression [dB]</i> . . . . .	53
11	<i>AM: Contrast-to-Tissue-Ratio [dB]</i> . . . . .	54
12	<i>PIAM: Contrast-to-Tissue-Ratio [dB]</i> . . . . .	54
13	<i>PI: Contrast-to-Tissue-Ratio [dB]</i> . . . . .	55
14	<i>AM: Contrast-to-Noise-Ratio [dB]</i> . . . . .	55
15	<i>PIAM: Contrast-to-Noise-Ratio [dB]</i> . . . . .	55
16	<i>PI: Contrast-to-Noise-Ratio [dB]</i> . . . . .	56

# Abbreviations

<b>AM</b>	Amplitude Modulation
<b>AM filter</b>	Filter used instead of constant downscaling factor ( $\alpha$ ) in AM
<b>C</b>	Contrast
<b>CNR</b>	Contrast-to-Noise-Ratio
<b>CTR</b>	Contrast-to-Tissue-Ratio
<b>FEC</b>	Front End Controller
<b>GE</b>	General Electric
<b>HV</b>	High Voltage
<b>I</b>	Intensity
<b>IQ</b>	In-phase Quadrature
<b>MI</b>	Mechanical Index
<b>PI</b>	Pulse Inversion
<b>PIAM</b>	Pulse Inversion and Amplitude Modulation
<b>PRF</b>	Pulse Repetition Frequency
<b>RF</b>	Radio Frequency
<b>US</b>	Ultrasound
<b>T</b>	Tissue
<b>TS</b>	Tissue Suppression

# 1 Introduction

Ultrasound combined with infusion of contrast agent has been used to image myocardial perfusion for the last decade, but this does not work satisfactory for all patients. The imaging is hard to perform as the blood arteries in the myocardium are extremely small and have very low blood velocities compared to the motion of the hart muscle. At the same time is the ability to discover reduced perfusion very important, both to be able to detect coronary diseases at an early stage and to diagnosticate the amount of reduced hart function.

The main reason to use contrast agent in ultrasound blood imaging is the strengthened backscattered signal. Without employing contrast agent is the echo intensity from blood approximately 30-60 dB below the intensity from the surrounding tissue. But the bubbles in the agent do not only increase the intensity in the signal, they also introduce nonlinearities in the echoes. This nonlinear scattering effect is utilized to distinguish contrast signal from the linear tissue signal. One way to do this is by transmitting two pulses of opposite polarity and sum the echoes of the pulses to create an image, pulse inversion (PI), which is the method used on the GE Vingmed Ultrasound scanner today. Employing PI produces nonlinear echoes from the contrast bubbles which are located at twice the transmitted frequency, i.e. the 2<sup>nd</sup> harmonic. Other multi-pulse techniques enhance the nonlinear bubble echoes by transmitting pulses of different power, amplitude modulation (AM). This results in echoes both having nonlinear signal on the fundamental and the 2<sup>nd</sup> harmonic frequency, however the 2<sup>nd</sup> harmonic part is not as large as in PI. A combination of both techniques (PIAM) would furthermore have the advantage of both gaining a stronger 2<sup>nd</sup> harmonic component than AM and a fundamental component which is not present in PI [12].

When a multi-pulse technique is employed to increase the nonlinear signal from contrast bubbles, it is just as important to suppress the linear signal from tissue. The motivation of this thesis is to improve techniques which utilize pulses of different amplitude by first and foremost reducing the tissue signal.

The reader is given an introduction to ultrasound imaging and further to the use of contrast agent in the second chapter of this thesis. A detailed description of experimental acquisitions and post processing of ultrasound data are presented in the following chapters. The obtained results are reproduced and commented in chapter 5, before they are analyzed and discussed in chapter 6. Based on the discussion, a suggested new imaging technique and the main conclusions are given in the last chapters. The document does furthermore include a bibliography and an appendix where more detailed tables of the results can be found.

## 2 Theory

### 2.1 Ultrasound Imaging

In diagnostic ultrasound imaging an acoustical pressure pulse, generally in the frequency range 1-10 MHz, is generated and transmitted into the body. When the pulse propagates through tissue it is partly reflected as a consequence of inhomogeneities, i.e. changes in density and compressibility in the tissue. This reflected part of the pulse is received and utilized to construct an image of a region inside the body.

#### 2.1.1 Basic principle of Ultrasound Imaging

The ultrasound imaging process starts with the generation of an electrical pulse which is applied to a transducer. The transducer converts the electrical pulse into an acoustical pulse to be transmitted into the body. When the reflected part of the pulse is received it affects the transducer to start vibrating. These vibrations are converted back to an electrical pulse.

Several pulses are transmitted in different directions to make an image of a region. In order to image various depths are the backscattered echoes from a single pulse sampled a number of times. Which depth each echo is originated from is decided by the time after the pulse transmission. Given the sound propagation velocity  $c$  and the time  $t$ , is the distance given by  $r = tc/2$ . The time delay from the pulse is transmitted to the echoes are received limits how frequently pulses can be generated in order not to mix echoes from different depths. The maximum pulse repetition frequency (PRF) is thus  $c/2r_{max}$ .

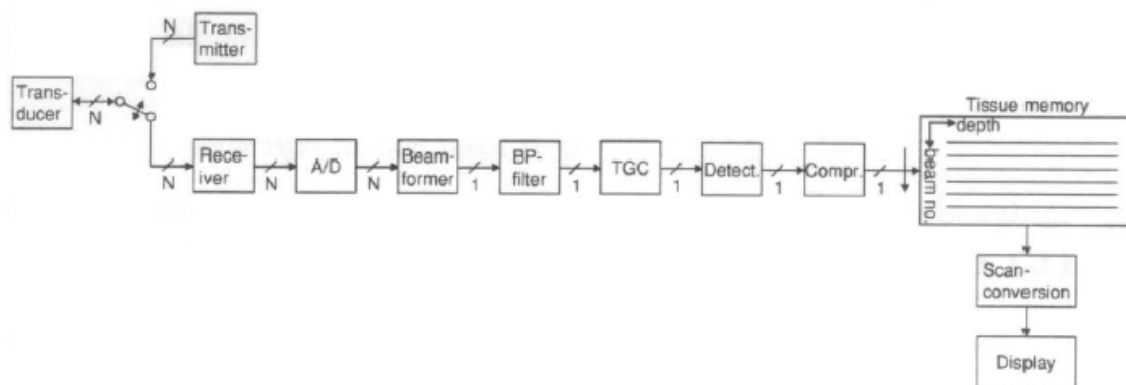


Figure 1: *Ultrasound imaging system* [14]

The pulse is attenuated during propagation through tissue. This attenuation is of course higher for echoes from deeper structures than those originating from shallower structures. To compensate for this different attenuation, the signal is amplified with a gain that increases with time, i.e. higher amplification for echoes from greater depths. This process is known as time gain compensating (TGC). After TGC the envelope of the signal is calculated, before the signal is logarithmic compressed in order to visualize both strong and weaker echoes in the same image. The image could then be displayed with time (ranges) vertically and beam number (width) horizontally.

More details of ultrasound imaging principles can be found in [1] and [5].

### 2.1.2 IQ demodulation

RF-data (radio frequency data) is used to denote unprocessed data. The term is adopted from radio communication as the signal contains information in the frequency bands used for radio communication. In an ultrasound scanner RF-data is known as the output of the beamformer. The RF-data is converted to a complex representation, IQ-data, which is an abbreviation for In-phase Quadrature data. This is described more detailed in [6].

The RF-data from an ultrasound transducer is a band-pass signal which is sampled at a sufficient high level to meet the Nyquist limit and thus avoid aliasing. The main reason to perform IQ demodulation is to reduce the sampling frequency and therewith reduce the amount of data without losing essential information. The demodulation is done by first moving the frequency band to be centered on zero frequency, this step is called down-mixing. Then the complex signal is low-pass filtered in order to remove the negative frequency band. The filtering process does of course also remove noise outside the desired band. At this point the maximum frequency of the signal is reduced. This also reduces the Nyquist limit and the requested sampling frequency. So, to reduce the sampling frequency, down-mixing of the signal is preformed.

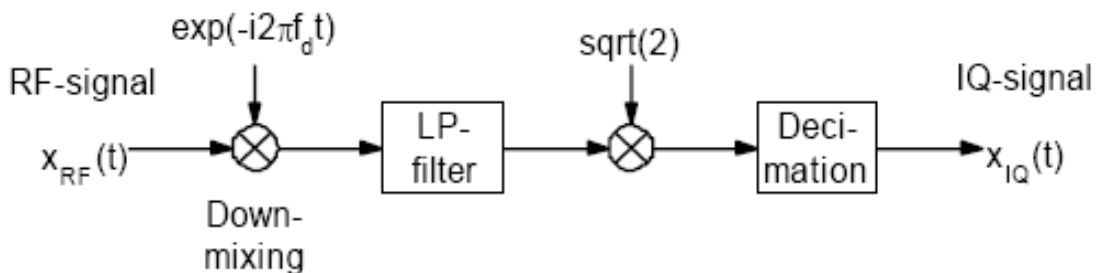


Figure 2: IQ demodulation [6]

Figure 2 illustrates the IQ demodulation process. The multiplication with  $\sqrt{2}$  is done in order to preserve the signal energy when the negative part of the frequency band is removed.

### 2.1.3 The Mechanical Index (MI)

The mechanical index is defined as negative peak pressure in MPa divided by the square root of the frequency in MHz [2]:

$$MI = \frac{P_{neg}}{\sqrt{f}} \quad (1)$$

This measurement reflects the normalized energy which a target is exposed to in an ultrasound field. The maximal MI allowed in a clinical examination is 1.9. But MI is not only important for safety reasons, the quantity is also an influential factor in contrast imaging. This is due the various behaviors of contrast bubbles when it is exposed to different pulse energies.

## 2.2 Image quality in ultrasound

The quality of an ultrasound image is mainly described by two factors; spatial and contrast<sup>1</sup> resolution [1].

### 2.2.1 Spatial resolution

The spatial resolution of an ultrasound image is divided in two measurements, radial and lateral resolution.

#### Radial resolution

The radial resolution reflects the ability to distinguish two objects along the beam axis, given by [5]:

$$\Delta r = \frac{cT_p}{2}, \quad (2)$$

where  $T_p$  is the pulse length and  $c$  is the speed of sound. A short pulse will thus provide a better radial resolution than a longer. The echoes from two objects along the beam

---

<sup>1</sup>Contrast resolution must not be confused with the use of contrast agent.

direction will overlap if they are located too closely, and this is obvious a greater problem for longer pulses. A short pulse will though have higher frequency (the number of periods is usually constant), this will cause a higher attenuation of the pulse. Thus, there is a trade off-between between radial resolution and penetration depth. Another drawback using a shorter pulse is the wider frequency band which increases the noise level in the image.

### **Lateral resolution**

The lateral resolution reflects the ability to distinguish two objects in the lateral direction, i.e. two objects in the same depth with a horizontal distance between one another. This is expressed by the Rayleigh-criteria [10]:

$$\Delta L = \frac{Fc}{Df}, \quad (3)$$

where F is the distance from the transducer to the focal point, D is the length of the aperture (i.e. the width of the elements used in the transducer) and f is the transmitted frequency. According to (3) can the lateral resolution be improved by increasing the aperture, but this will limit the ability of the beam passing between bone structures, for instance the ribs in cardiology. Increased frequency will improve the lateral resolution like the radial resolution.

### **2.2.2 Contrast resolution**

The contrast resolution describes the ability to detect small variations in the intensity of the back-scattered signal from closely located targets. Signal generated noise is the main limitation of the contrast resolution, which is caused by sidelobes and reverberations. Electronic noise in the transducer will have an affect on the contrast resolution as well [1].

### **Sidelobes**

In the ideal case would the intensity of each sample of the received echo signal merely be decided by the reflections from the main lobe of the transmitted wave. However the sidelobes will unfortunately contribute signals from other directions than the intended one. Thus, reflectors nearby a position of imaging will be registered as weaker reflectors in the position, and therefore deteriorate the image quality. Hence, it is desirable to have as low sidelobe level as possible, in order to obtain as good contrast resolution as possible. The sidelobe can be diminished by apodization. This is achieved by reducing the signal



from the outer elements of the probe. But the drawback by apodization is the increased width of the main lobe which reduces the lateral resolution.

### Reverberations

Reverberations are multiple reflections of the transmitted pulse. This occurs when a pulse propagates through several boundary surfaces, and is reflected back and forth between the surfaces. Consequently will the multiple echoes reach the receiver later than the original echoes from the same depth, and thus create an artifact which is displayed farther down in the image, or the reverberations might even interfere with the echoes of the next pulse.

## 2.3 Ultrasound contrast imaging

The echo signal from blood has 30-40 dB lower intensity compared to the signal from the surrounding tissue. This makes it almost impossible to image small blood vessels with little flow and very low blood velocity (i.e. capillaries) without the use of a contrast agent. The agent, which is injected into the blood, both increases the intensity of the backscattered signal and introduces nonlinearities in the signal.

### 2.3.1 The contrast agent

The contrast agent used in ultrasound imaging contains small gas-filled bubbles with diameter 3 – 5  $\mu\text{m}$ . This means that they are smaller than the red blood corpuscles (about 7  $\mu\text{m}$ ) and thus passes through even the smallest capillary blood vessels. The agent has to meet some other specifications too [2]. The bubbles have to be stable in the in the blood a period of time for them to reach the area of interest, and the agent can naturally not be poisonous.

### 2.3.2 Scatters from contrast agent

The reason for the strong backscattered signal from the contrast agent is the large difference in acoustical impedance between the bubbles and the surrounding fluid. And also when the bubbles are exposed to ultrasound, they start to oscillate. These oscillations are at maximum at the resonance frequency, which is decided by the size and the stiffness of the bubble. The resonance frequency for an encapsulated contrast bubble is given by [2]:

$$f_b = \frac{1}{2\pi a} \sqrt{\frac{3\gamma p_0 + 12G_s d_{Se}/a}{\rho_0}}, \quad (4)$$

where  $\gamma$  is the ideal adiabatic gas constant,  $\rho_0$  is the surrounding medium density,  $p_0$  is the pressure in the medium,  $G_s$  is the modulus of rigidity and  $d_{se}$  is the shell thickness. At this frequency is the scatter cross-section of the bubbles at its peak value, which result in maximum energy in the echo signal. The relatively large size of the contrast bubbles does however result in a rather high value of  $f_b$ , which lies outside the pass-band of the probe, and a transmission at this frequency would anyway lead to an unacceptable high attenuation. Thus is the frequency employed in contrast application somewhat lower compared to  $f_b$ .

The resonant oscillation of the bubbles does also introduce nonlinearity in the backscattered signal. The Rayleigh-Plesset equation [1] gives a mathematical model of the nonlinear bubble oscillation:

$$\rho(a\ddot{a} + \frac{3}{2}\dot{a}^2) = p(a, t) - p_0 - p_i(t), \quad (5)$$

where  $p_0$  is the surrounding pressure,  $p(a, t)$  is the bubble surface pressure and  $p_i$  is the pressure of the incoming wave. In the far field is the scattered field given by (6). The equation shows how the harmonic components are generated.

$$p_s(r, t) = \frac{\rho}{r}(a^2\ddot{a} + 2a\dot{a}^2) \quad (6)$$

The nonlinearities, which cause the harmonics, arise as a consequence of the expansion and the contraction of the bubbles being asymmetric at sufficient high pressure. The asymmetric oscillation moves parts of the signal from the fundamental frequency to higher harmonics. When the bubbles are exposed to a low pressured pulse ( $MI < 0.1$ ) [5] they will oscillate similar to the pulse, which gives a linear backscattered signal. As the  $MI$  increases, the bubbles start to oscillate asymmetric which introduces nonlinearities and thus harmonic frequency components in the signal. If the pressure is increased even further ( $MI > 1$ ) will the bubbles be destroyed and produce a powerful backscattered signal with strong harmonic components. The echoes from tissue do also

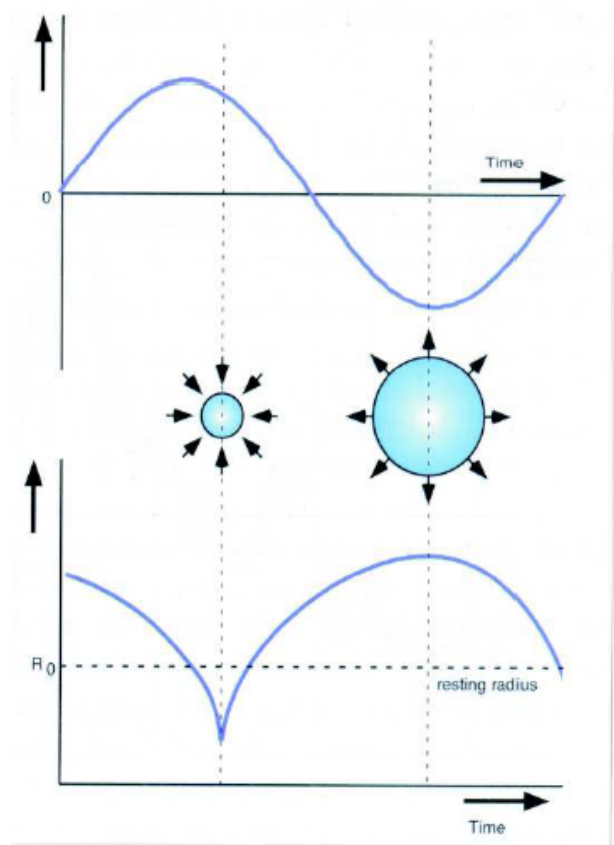


Figure 3: Asymmetric oscillation of an ultrasound contrast bubble [2]

contain harmonic components, but these are at a much lower level. This is utilized in contrast based imaging techniques [2].

### 2.3.3 Non-linear propagation in tissue

High power acoustical pressure in the transmitted ultrasound waves introduces nonlinearities in the waves during propagation. This causes a change in the shape of the waves as it propagates through tissue. The reason why this occur is the rapidly change in the substance density caused by the high intensity wave, which further will result in a change in the speed of sound. The perturbed speed of sound can be expressed by Beyer's equation [11]:

$$c(t) = c_0 \left( 1 + \frac{1}{2} \frac{B}{A} \frac{U(t)}{c_0} \right)^{\frac{2A}{B} + 1} \quad (7)$$

$c_0$  is the speed of sound for a linear wave,  $\rho_0$  is the density of the undisturbed medium and  $U(t)$  is the particle velocity. The ratio  $B/A$  is an indication of how the medium supports the generation of nonlinear waves. A high  $B/A$  value will thus result in a large generation of nonlinearities. Typical values of  $B/A$ -ratio are given in table 1. Fat does give a stronger nonlinear response compared to fluids like water and blood.

Table 1: *Typical B/A values*

Water	4.2-6.1
Blood	6.3
Fat	11.1

Equation (7) shows that a positive particle velocity  $U(t)$  results in a faster propagation velocity  $c(t)$  than  $c_0$ , while a negative  $U(t)$  gives  $c(t) < c_0$ . The positive pressure amplitude will therefore propagate faster than the negative, which results in a power shift from the negative to the positive amplitude. This deformation will for instance lead to a saw tooth formed wave if the transmitted pulse has a sinus. In figure 4 is this phenomenon illustrated. Also notice the change in the frequency spectrum, where energy is moved from the fundamental frequency to harmonic components.

Harmonic components can also arise when a wave is backscattered, which occurs when contrast agent is used as described in the previous section.

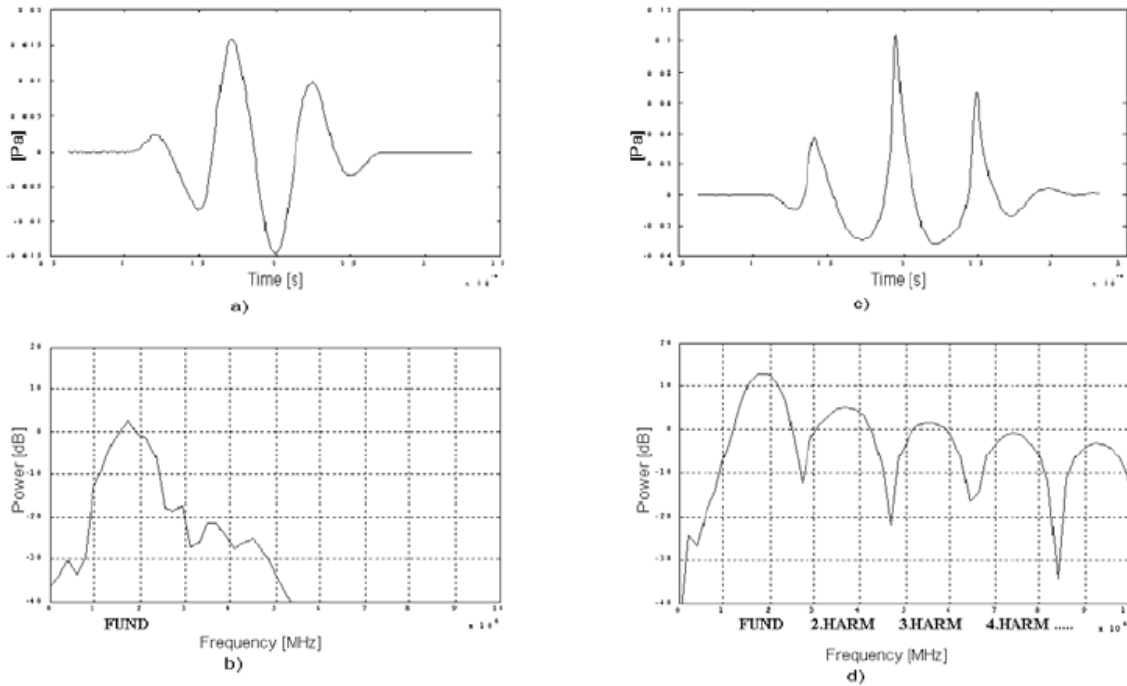


Figure 4: A transmitted pulse (a) and its frequency spectrum (b). The pulse is deformed after propagation(c), and harmonic components have arisen (d). The figure is from a presentation of Prof. Hans Torp, IFBT, NTNU.

## 2.4 Detection techniques of ultrasound contrast bubbles

The main concept behind ultrasound contrast imaging is to enhance the nonlinear signal from the bubbles, and, at the same time, suppress the linear signal from surrounding tissue. In this section are three different two-pulse techniques described; pulse inversion (PI), amplitude modulation<sup>2</sup> (AM), and the combination PIAM.

### 2.4.1 Pulse inversion

In pulse inversion (PI) [5] two similar pulses with opposite polarity are transmitted. When adding the echo from the pulses on receive, all the linear components should be removed. More accurate will all odd harmonic frequency components be cancelled, while the even harmonic components are increased by a factor 2. This means in practical, with a limited

<sup>1</sup>Amplitude modulation is also known as power modulation (PM)

transducer bandwidth, that the fundamental frequency component is suppressed and the  $2^{nd}$  harmonic component enhanced. The method could thus be viewed as a band-pass filter centered at twice the transmitted frequency. Equation (8)-(10) describes this process.  $p_1$  and  $p_2$  are the transmitted pulses, while  $e_1$  and  $e_2$  are the corresponding echoes.

$$p_2(\vec{r}, t) = -p_1(\vec{r}, t - \tau) \quad (8)$$

$$e_1(\vec{r}, t) = Echo[p_1(\vec{r}, t)], \quad e_2(\vec{r}, t) = Echo[p_2(\vec{r}, t)] \quad (9)$$

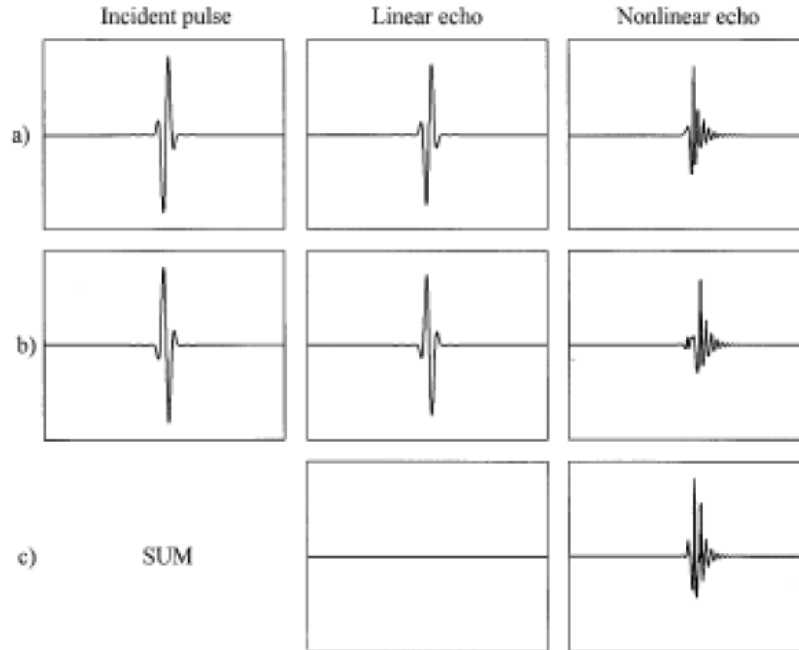
$$p_i = e_1 + e_2 \quad (10)$$

The main reason why PI performs significantly better than an ordinary single pulse technique is, as mentioned earlier, the contrast agent bubbles providing an echo signal containing far more nonlinearities than the echo signal from tissue. This results in a greater cancellation of tissue signal compared to the signal from contrast bubbles when the echoes from two equal transmitted pulses with opposite polarity are added. Employing PI will clearly increase the Contrast-to-Tissue-Ratio (CTR). Also the Contrast-to-Noise-Ratio (CNR) will be improved since two pulses are used instead of one. Another advantage PI provides compared to a single transmitted pulse and a  $2^{nd}$  harmonic filter on receive, is that the entire bandwidth on the received echo signal can be used, which improves the spatial resolution. However in practical use is a  $2^{nd}$  harmonic filter employed also in PI, in order to improve the contrast resolution by removing e.g. reverberations at the fundamental. But a multi pulse technique like PI has a quite significant disadvantage in the sensitivity to motion. And also the frame rate is of course reduced by a factor of two when two pulses are transmitted in the same direction instead of one.

### 2.4.2 Amplitude modulation

The idea behind amplitude modulation (AM) [8] is quite similar to PI. Instead of inverting the polarity between the two pulses, the second pulse in AM is an amplitude adjusted copy of the first one. When the echoes are received the amplitude difference will be compensated before the second echo signal is subtracted from the first one, to remove the linear scattering. This is shown in equation (11) and (12), where  $\alpha$  is the amplitude adjusting factor.

$$p_2(\vec{r}, t) = \alpha p_1(\vec{r}, t - \tau), \quad \alpha \in (0, 1) \quad (11)$$

Figure 5: *Pulse inversion* [13]

$$am = e_1 - \frac{1}{\alpha}e_2 \quad (12)$$

The advantage of AM compared to PI is the ability to detect pressure dependent nonlinear effects [3]. This leads to conserving of the odd harmonic components in the processed echo signal. You might think this would not affect the signal at all, since the lowest odd harmonic is the 3<sup>rd</sup> ordered which is outside the pass-band of the probe. But, in fact, the 3<sup>rd</sup> order nonlinear component gives a contribution to the fundamental frequency. This means that there is some nonlinearity at the fundamental frequency, which makes it possible to do the imaging at the fundamental. If this is done it is no longer essential to receive the 2<sup>nd</sup> harmonic and the transmitted frequency is thus not limited to the lower parts of the probe. But this modulation technique has a quite considerable drawback. Imaging at the fundamental makes the reverberations more evident. Disadvantages mentioned for PI, like the reduced frame rate and sensitivity to motion, are drawbacks here as well. It is however possible to reduce the sensitivity to motion by removing the phase information in the backscattered signal. This is done by subtracting the absolute value of the echoes, instead of the complex value, which removes the phase shift caused by the tissue motion. But doing so will also eliminate phase changes caused by nonlinear scattering, which will

decrease the CTR and weaken the method.

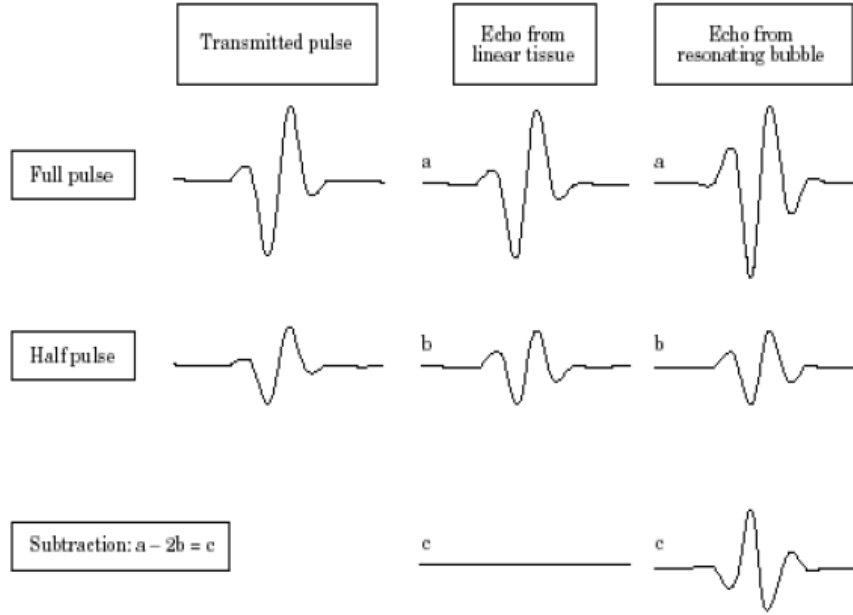


Figure 6: *Amplitude modulation* [15]

### 2.4.3 Combination of PI and AM

It is also possible to use a combination of PI and AM (PIAM) [9]. In this case two pulses with opposite polarity and different amplitude are transmitted. The received signals will be added with amplitude compensation in order to remove as much linear signal as possible.

$$p_2(\vec{r}, t) = -\alpha p_1(\vec{r}, t - \tau), \quad \alpha \in (0, 1) \quad (13)$$

$$p_{iam} = e_1 + \frac{1}{\alpha} e_2 \quad (14)$$

Combining PI and AM will result in a stronger  $2^{nd}$  harmonic component from the contrast bubbles compared to a pure AM technique [12]. The only drawback using PIAM over AM is the lack of possibility to remove phase information to reduce the effect of tissue motion as in AM. PIAM imaging could both be used in the fundamental, the  $2^{nd}$  harmonic or as a full-band technique.

### 3 Measurements

This chapter describes the data acquisition done in the diploma work. The measurements include measurements of electrical and acoustical pulses, and also the acquisitions of iq-data done on a flow phantom with contrast agent and on a tissue phantom.

#### 3.1 Electrical pulses

The electrical pulses were measured by connecting an oscilloscope to the TX-board on the ultrasound scanner. The oscilloscope was further connected to a computer, using Matlab based software. Triggng of the oscilloscope was done by connecting it to the Front End Controller (FEC) of the scanner, where the transmit trigger signal is sent to the TX-card.

The Matlab based software on the computer converted the signal from the oscilloscope to Matlab compatible data. Each recorded electrical pulse is an average over 64 pulses in order to remove noise signal from the pulse. To be able to calculate the average over several pulses, all pulses had to be transmitted with the same delay. This was achieved by setting the scanner in M-mode and use 2D-freeze.

Table 2: *Equipment used meassuring electrical pulses*

<b>Equipment</b>	<b>Fabrication</b>	<b>Type</b>
Ultrasound scanner	GE Vingmed Ultrasound AS	Vivid7
Oscilloscope	LeCroy	LT262
Software	IFBT, NTNU	Lab Application version 1.5, 2000

#### 3.2 Acoustical pulses

The acoustical pulses were measured by using a hydrophone in a water tank. The ultrasound probe was first fastened with a clamp, before the hydrophone was adjusted to the right position by a stepper motor. The motor was able to do step down to 1 mm, and the hydrophone was moved around to find the center of the probe, i.e. where the measured pulse had its maximum value. As for the electrical pulses was an oscilloscope used to perform the measurements, and the triggng was done by connecting the scope to the FEC. Each pulse finally stored on the computer was averaged over 128 pulses to eliminate noise signal.

The measurements were performed in a distance of 5 mm from the probe, i.e. the near field of the beam. This is due to the nonlinear properties of water and the demand of



measuring the exact transmitted pulse. Furthermore the aperture was set down, so the probe transmitted only using a single element.

It was very important to avoid air bubbles in the water during the measurements. If this occurred it would cause significant distortions in the sound beam. The problem was avoided by first using degassed water in the tank, and second by squirting water with a syringe on the hydrophone and the transducer surface.

Table 3: *Equipment used measuring acoustical pulses*

<b>Equipment</b>	<b>Fabrication</b>	<b>Type</b>
Ultrasound scanner	GE Vingmed Ultrasound AS	Vivid7
Probe	GE Vingmed Ultrasound AS	3.5MHz M3S 1.5D phased array
Oscilloscope	LeCroy	LT262
Hydrophone	Precision Acoustics Ltd.	2 mm, Serial no. 1088
Software	IFBT, NTNU	Lab Application version 1.5, 2000

### 3.3 Acquisition of phantom data

The experiments were performed in vitro on a flow phantom which is a model made of a tissue mimicking material. All data were acquired using a Vivid7 ultrasound scanner and the M3S probe.

Inside the phantom there is an 8 mm flow channel. The phantom was connected to a flow system consisting of a bucket containing 0.1 ml contrast agent in 2 l water, a magnetic stirrer which mixed the contrast solution and an electric roller pump to make the fluid flow inside the pipe of the phantom. To keep the probe steady during the experiment a stand with a clamp was used. The setup can be viewed in figure 7.

Table 4: *Equipment used in the acquisition of flow phantom data*

<b>Equipment</b>	<b>Fabrication</b>	<b>Type</b>
Ultrasound scanner	GE Vingmed Ultrasound AS	Vivid7
Probe	GE Vingmed Ultrasound AS	3.5MHz M3S 1.5D phased array
Flow phantom	ATS Laboratories, INC	523A
Pump	Multifix	Electric roller pump
Contrast agent	GE Healthcare AS	Optison
Contrast agent	GE Healthcare AS	Sonazoid
Magnetic stirrer	Stuart	SB161

Figure 7: *Experimental setup*

### 3.3.1 Scanner settings

Rectangular pulses with pulse length 2.5 and 3.5 periods were used during the acquisition. The pulses were transmitted with a PRF (pulse repetition frequency) of 3 kHz and decimation factor 5, i.e. a sampling frequency of  $\frac{20\text{MHz}}{5} = 4$  MHz for the IQ-data. The acquisition was done with frequency 1.5 MHz which is in the lower part of the pass-band of the probe, this was done in order to get both the fundamental and the 2<sup>nd</sup> harmonic component from the received echoes. In each direction a packet of 5 pulses was transmitted, in order to compare different modulation techniques on the measurements later on. Pulse 3 was amplitude modulated and pulse 4 was inverted, while both modulations were applied to pulse 2. The fifth pulse was added as a reference pulse relative to the first pulse. This gives the pulse packet:

$$T_x = [1 \quad -\alpha \quad \alpha \quad -1 \quad 1] \quad (15)$$

### 3.3.2 Reverberation problem

When the iq-data from the first measurement on the flow phantom were processed a problem was detected. Pulse 1 and 3 in the pulse packet given in (15) were employed in amplitude modulation, but this seemed to give a rather poor tissue suppression. A great effort was put into reveal the source of this defect, before pulse 5 and 3 were tested out for AM instead. This gave considerable better tissue suppression, which lead to the suspicion that reverberations could be the source of the error. To investigate this in more detail, several measurements on the flow phantom were performed. All measurements had different pulse packets:

$$T_x = [\underline{\alpha} \quad \underline{1}] \quad (16)$$

$$T_x = [\alpha \quad \underline{\alpha} \quad \underline{1}] \quad (17)$$

$$T_x = [\alpha \quad \underline{\alpha} \quad 1 \quad \underline{1}] \quad (18)$$

$$T_x = [\underline{1} \quad -\underline{1}] \quad (19)$$

In the four packets were the underlined pulses used in amplitude modulation (or pulse inversion for the last measurement given in (19)). The other pulses were added as reverberation pulses in order to study the effect these had on the echoes from the next pulses, which were used in the imaging. The last pulse packet was included to observe the absence of the problem in pulse inversion.

### 3.3.3 Acquisition

Something had to be done to avoid the problem with reverberations from one pulse which interfered with the echoes from the next pulse. The solution was to make sure that any two pulses used in a modulation technique did have the proportional same pulses in front of them. This would make the reverberation part in the two pulses at the relatively same level, which would suppress the reverberations in the same manner as the other parts of the linear tissue signal. The pulse packet employed in the new measurements is given in (20). For instance are pulse 3 and 5 used in AM. Since both pulses have a pulse in front with the same amplitude and opposite polarity (they could also have both the same polarity) will the reverberations be reduced significantly after the modulation technique is applied.

$$T_x = [1 \quad -1 \quad 1 \quad -\alpha \quad \alpha] \quad (20)$$

The data were acquired with four different transmit powers (5V, 6.08V, 7V and 10V). The transmitted power at exactly 6.08V was employed to be able to comparing PI and AM where the two pulses in both methods had the same average energy. Thus, PI would consist of two pulses with 6.08V, while AM (or PIAM) would have one pulse at 5V and one at 7V. The power modulation factor determines the amplitude of the amplitude modulated pulse ( $\alpha$  in (20)) compared to the pulse with full amplitude. This was set to -4.3 dB during the acquisitions, which gives AM pulses at 3.79V when the transmitted power is set to 5V, 4.45V for 6.08V, 5V for 7V and 6.84V for 10V.

It was important to avoid air bubbles in the flow system during the experiment. Air bubbles would cause a strong backscattered signal and thus interfere with the echoes from contrast bubbles. To get rid possible air in the circuit the pump was running for several minutes before the measurements were performed.

Another issue of importance is the concentration of contrast bubbles which should be equal for each measurement. This is important to be able to compare modulation techniques for different transmitted powers, different contrast agents and different pulse lengths. A variation in the concentration would cause a change in the intensity of the echo signals, and thus make an unfair assessment. The most suited way to avoid this from happening is to use an infusion pump to constantly inject contrast agent close to the phantom. But this would also cause a motion of the fluid, which produces a phase shift in the echoes from two following pulses. If this occurs it would make it hard to distinguish which nonlinearities were caused by the pulse modulation and which by motion of contrast bubbles. So, to make the contrast concentration as equal as possible the roller pump was activated for 20 seconds between each measurement to get fresh contrast into the phantom pipe, and then switched off for 10 seconds, before the data were recorded. Half way through the experiment the pump was made running for a while when the scanner transmitted high powered pulses to destroy the remaining contrast bubbles, before new contrast agent was added to the circulating fluid.

### 3.3.4 Tissue phantom

The same measurements performed on the flow phantom were done on a tissue phantom too. The intention to do this was to make AM filters from the phantom data. See section 4.4 for details about the filter.

Table 5: *Equipment used in the acquisition of tissue phantom data*

<b>Equipment</b>	<b>Fabrication</b>	<b>Type</b>
Ultrasound scanner	GE Vingmed Ultrasound AS	Vivid7
Probe	GE Vingmed Ultrasound AS	3.5MHz M3S 1.5D phased array
Tissue phantom	CIRS	General Purpose Multi-Tissue Ultrasound Phantom, Model: 040

## 4 Processing of IQ-data

The IQ-data acquired on the US scanner were further analyzed and processed on a computer by Matlab programs developed by the author, in combination with the use of the Matlab program GCMat (GE Vingmed Ultrasound AS). GcMat is a custom made program to investigate and process ultrasound IQ-data.

### 4.1 IQ-data

The IQ-data, which are described in 2.1.2, are organized in four dimensions. During acquisition a number of pulses are transmitted in each beam direction. This number is denoted as the *packetsize*. When the transducer receives echoes from the reflectors, the echoes are sampled. The sample number is equal to a depth and indicated with a *range*. The scanning is then done in several directions or *beams*. This gives a scan plane, or a frame, consisting of *packets*  $\times$  *ranges*  $\times$  *beams*. During a measurement this process is repeated several times which produces a number of *frames*.

The measurements done here have *packetsize* 5, the number of *ranges* is 519 and the *beam* number is 60. The number of *frames* varies from 12 to 23.

### 4.2 Region of interest

In order to compare the backscattered signals from contrast bubbles with echoes from a pure tissue area, a segregation of data is necessary. This was done by collecting the IQ-data from an area of 30 ranges and 30 beams inside the pipeline of the phantom, and from a similar tissue mimicking area at the same depth. This is illustrated in figure 8.

### 4.3 Validation of the constant AM factor

The AM factor ( $\alpha$ ), which is set on the scanner, defines the amplitude difference between the two electrical pulses generated on the  $T_x$  board when amplitude modulation is applied. The electrical pulses are then transformed to acoustical pressure pulses to be transmitted. This transformation is a nonlinear process which makes it impossible to calculate the exact amplitude of the transmitted pulses. A more serious problem does also occur in AM. The electrical pulse to be generated has a lower limit. This gives the modulation factor an upper limit, which is low when the amplitude of the pulse (the transmitted power) is low. This limitation causes a lower  $\alpha$  than specified when a low powered pulse is modulated with a high factor.

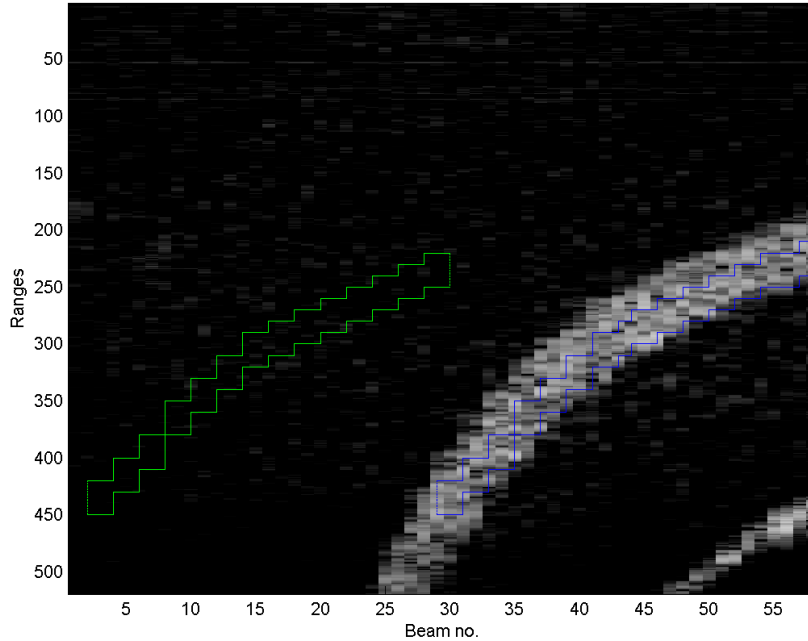


Figure 8: *Tissue* and *contrast* areas used in the analysis

To validate the actual  $\alpha$  the mean energy value of the iq-data from a tissue area for a transmitted pulse with full amplitude and an amplitude modulated pulse are compared. The ratio between these energy measures is used as a good indication of  $\alpha$ . A comparison of the two transmitted electrical or acoustical pulses could be another way to find the correct  $\alpha$ . But that has not been done in this work.

#### 4.4 The AM filter

The idea behind amplitude modulation is to utilize the nonlinear properties of the contrast bubbles to achieve echo signals from the bubbles. At the same time should the echoes from the surrounding tissue be suppressed as much as possible, see section 2.4.2. To make the suppression level of the linear tissue signal as high as possible a constant, which provides an optimal suppression, could be found, as described in the previous section.

After investigating the transmitted electrical pulses on the ultrasound scanner a weakness using a constant AM factor was revealed. Not only did the scanner not provide the exact amplitude as specified. Another more serious problem is the asymmetry between two pulses with different amplitude. This can clearly be seen both in the time domain and

the frequency spectra of the pulses. This indication was also confirmed by measurements of the acoustical pulses. Detailed results can be found in section 5.1.

As the scanner is not able to provide two equal pulses with different amplitude, a constant downscaling factor will not give a sufficient suppression. A way to compensate for this lack of symmetry is to generate a filter, which is used to compensate for different amplitude before subtraction, instead of the constant factor. Three different types of filters were tested out; a filter from the electrical pulses measured on the TX-card, a filter from acoustical pulses measured with a hydrophone in a water tank and finally a filter based on echo data from a tissue phantom.

#### 4.4.1 Filter from electrical pulses

The filter based on electrical pulses is made by the transfer function from the low-powered pulse to the high-powered pulse. In the frequency domain this is given as:

$$H_e(\omega) = \frac{P_{2e}(\omega)}{P_{1e}(\omega)}, \quad (21)$$

where  $P_1$  is the pulse with the highest power level. An example of two electrical pulses at 10 and 5 V is given in the upper part of figure 9. The lower part of figure 9 is the filter,  $H$ , in the frequency domain.

#### 4.4.2 Filter from acoustical pulses

The acoustical pulses were recorded with a hydrophone in a water tank, which is more detailed described in section 3.2. As for the electrical filter is the acoustical filter made by the transfer function from a pulse to another pulse with higher power. The acoustical filter is given in (22), and an illustration of two acoustical pulses and the filter constructed from these can be viewed in figure 10.

$$H_a(\omega) = \frac{P_{2a}(\omega)}{P_{1a}(\omega)}, \quad (22)$$

#### 4.4.3 Filter from tissue data

The third attempt to make a filter to improve the tissue suppression in amplitude modulation was to create a filter from echo data. The filter was made from iq-data acquired



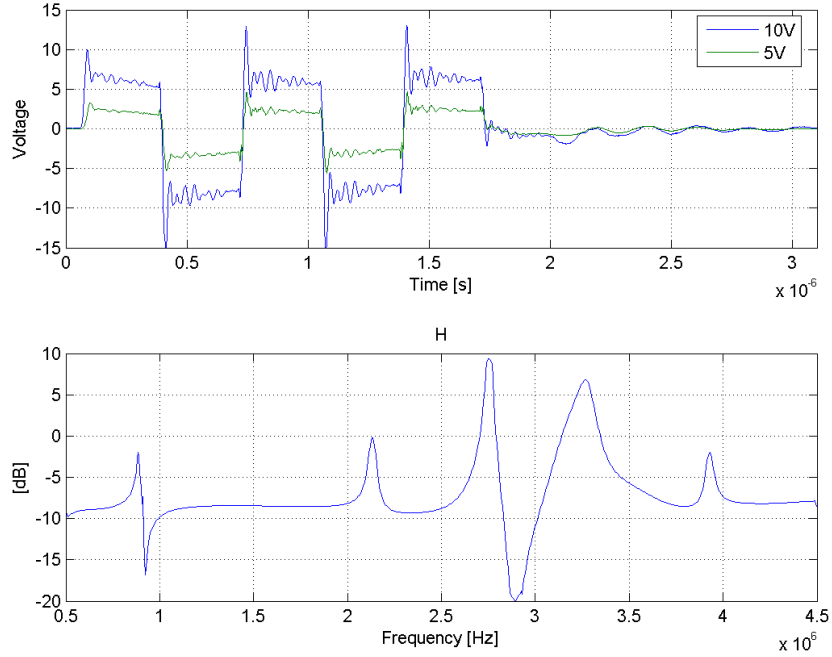


Figure 9: *Electrical pulses specified at 10 and 5 V (upper). Frequency spectrum of the filter from the electrical pulses (lower).*

from a tissue phantom. From the image of the phantom was an area, as homogeneous as possible, used. This is illustrated in figure 11. As can be seen from the figure is an area of 10 beams and 150 ranges (depth samples) utilized for the filter.

For each of the 10 beams a filter is created as:

$$H_t(\omega, n) = \frac{E_{2t}(\omega, n)}{E_{1t}(\omega, n)}, \quad n = 1, \dots, 10, \quad (23)$$

where  $E_{t1}$  and  $E_{t2}$  are the echo signals from the phantom, and  $n$  indicates the beam number. Then a single filter is made by calculating the mean value of all 10 filters:

$$H_t(\omega) = \langle H_t(\omega, n) \rangle_n \quad (24)$$

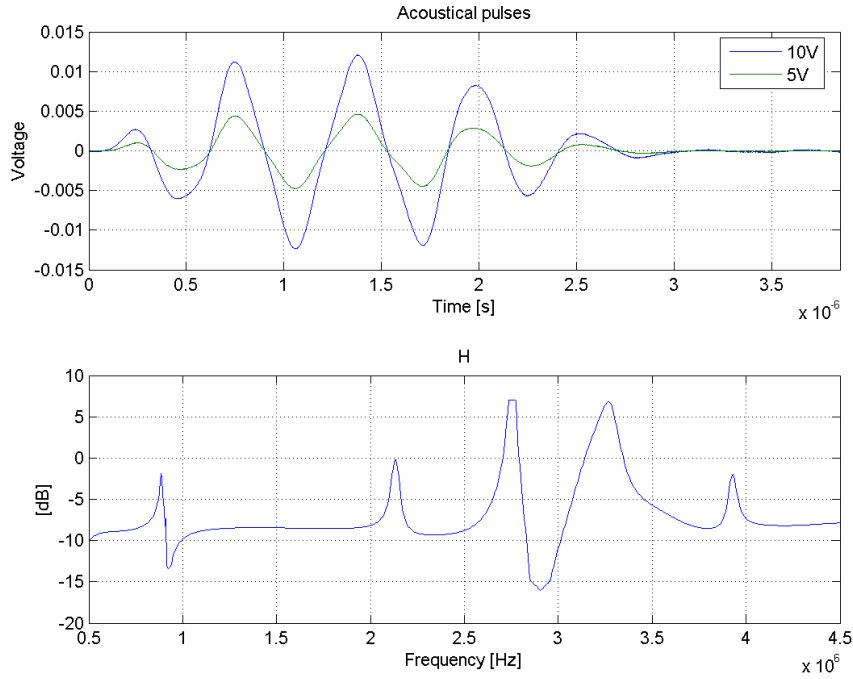


Figure 10: *Acoustical pulses specified at 10 and 5 V (upper). Frequency spectrum of the filter from the acoustical pulses (lower). Scaling: 12.2 MPa/V*

#### 4.4.4 Filter applied in AM

All three filters described above were tested out by applying them on data from a flow phantom. This made it possible to see how well the filters performed by measuring the tissue suppression and comparing it to the performance of AM with constant downscaling ( $\alpha$ ). At the same time the contrast signal had to be measured after the AM processing, to make sure that the filter did not decrease the contrast signal as much as the improvement of the tissue suppression. In that case the Contrast-to-Tissue-Ratio would not be enhanced, which is the main objective.

When the echoes from the two pulses are received the signal from the high-powered pulse will be filtered with one of the filters given in (21), (22) and (23). In the frequency domain this can be written as:

$$AM(\omega) = E_1(\omega) \cdot H(\omega) - E_2(\omega), \quad (25)$$

or in the time domain as:

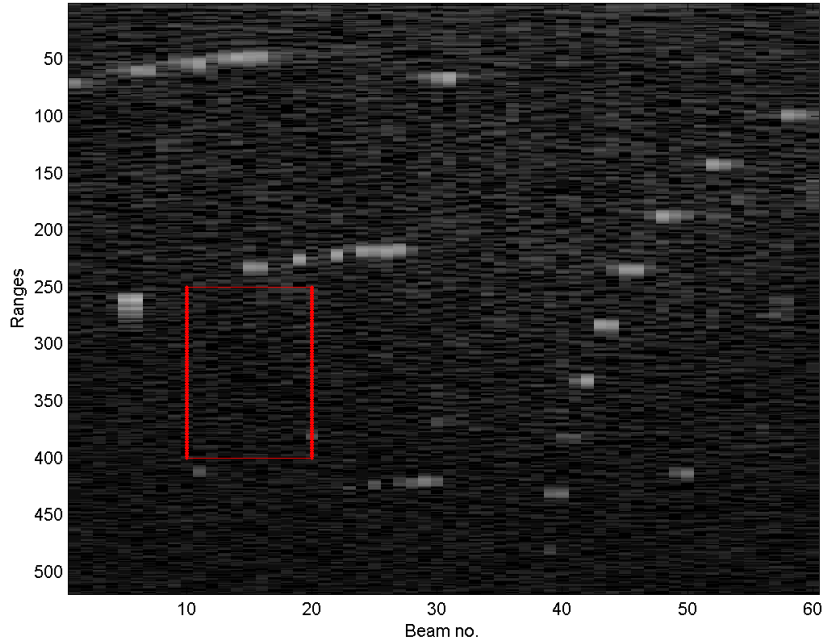


Figure 11: *The red frame indicates the region from the tissue phantom used to create the AM-filter.*

$$am(t) = e_1(t) * h(t) - e_2(t), \quad (26)$$

where  $E(\omega)$  is the echo signal in the frequency domain,  $e(t)$  in the time domain and  $*$  denotes the time convolution.

#### 4.4.5 Filter issues

During the development of the filters a great effort was put into making a filter which did not deteriorate the image quality. A good illustration of this problem can be seen in figure 12, where AM is applied in combination with a filter from tissue echoes. The filter used in this case is not modified more then described in 4.4.3. The filter does thus have the same length as the number of ranges of the area the filter is gathered from, i.e. 150. As can be observed from figure 12 does the frequency response of the filter alter rapidly, and the processed image is "smeared out".

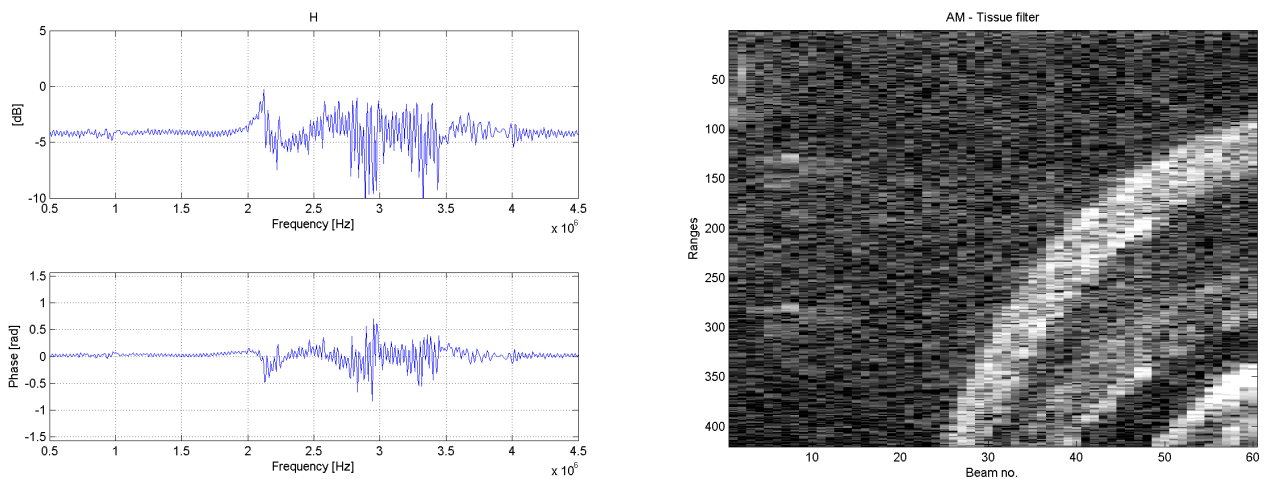
In figure 13 the filter length has been reduced to 25, by only using the 25 first filter coefficients. This seems to reduce the "smearing out" problem a good deal. And finally

in figure 14 the filter has been smoothed in addition. This is achieved by employing a moving average (MA-) filter, with length 5, to the filter. For the reader it can be difficult to see the effect of the MA-filter by comparing the images in figure 13 and 14. But if you look careful at the lower part of the pipeline with contrast agent in figure 13, is it possible to observe that the strong signal from the contrast bubbles also can be found right outside the pipeline. Furthermore you can notice the absence of this artifact in figure 14, where the MA-filter is employed.

The process of reducing the filter length and smoothening the filter is summarized in equation (27) and (28).  $h$  is the filter in time domain,  $H$  in frequency domain, and MA is the filter used for smoothening.

$$h = h(1 : 25) \quad (27)$$

$$H = H \cdot MA \quad (28)$$



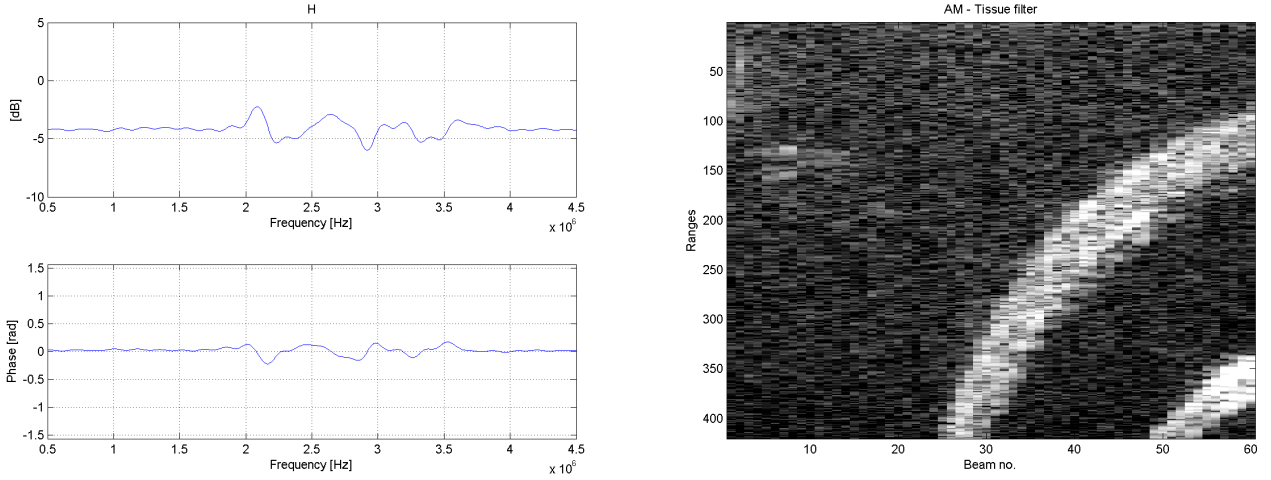
(a) Filter: frequency spectrum and phase response

(b) Image after AM with filter

Figure 12: Filter used in amplitude modulation. Filter length 150, no smoothing employed.

## 4.5 Quality measurement: CTR, CNR and TS

A straightforward way to quantify the quality of different techniques and scanner settings is to compute Contrast-to-Tissue-Ratio (CTR), Contrast-to-Noise-Ratio (CNR) and Tissue Suppression (TS). CTR is found by first getting the IQ-data from a contrast and a



(a) Filter: frequency spectrum and phase response

(b) Image after AM with filter

Figure 13: Filter used in amplitude modulation. Filter length 25, no smoothing employed.

tissue area, before the requested modulation technique and filtering are performed. The CTR is then measured by dividing the average intensity in the contrast data by the average intensity in the tissue data, which equals a subtraction in the logarithmic scale:

$$CTR_{dB} = \langle I_{dB}(C) \rangle - \langle I_{dB}(T) \rangle, \quad (29)$$

where C is the IQ-data from the contrast area and T is from the tissue area. The intensity,  $I_{dB}$ , is calculated as:

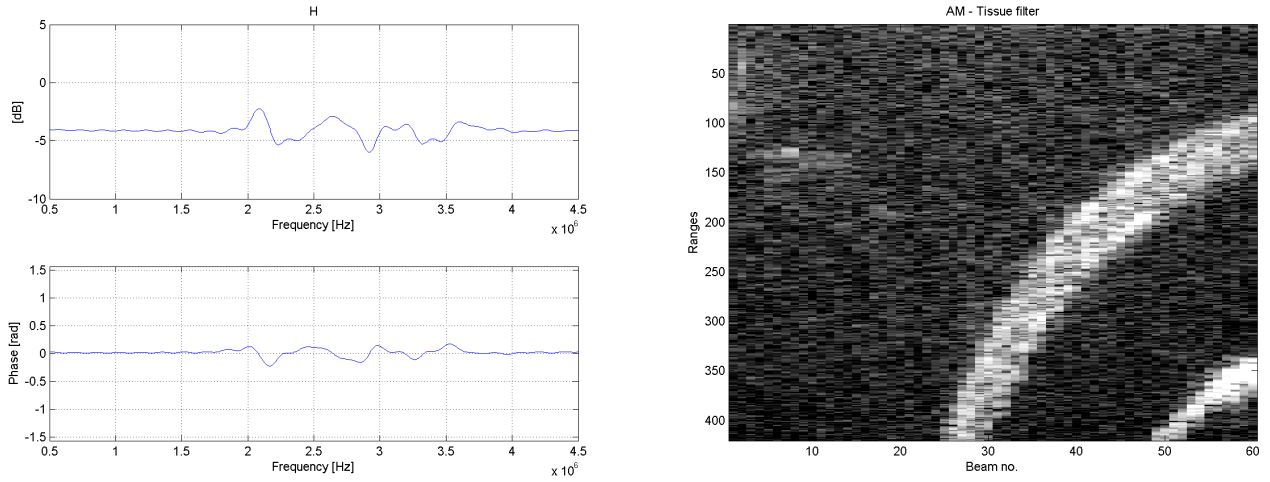
$$I_{dB} = 10 \log_{10}(|IQ|^2), \quad (30)$$

where IQ is the modulated IQ-data, e.g. PI (from the pulse packet given in (20)):

$$IQ_{pi} = IQ_{pulse2} + IQ_{pulse3}, \quad (31)$$

Calculating the CNR is done in an almost equal manner as CTR. The only difference is that the noise data, instead of tissue data, are compared with data from the contrast area. The noise data are collected from an area, equal to the contrast area, in a noise image, i.e. an image acquired without any transmitted pulses.

$$CNR_{dB} = \langle I_{dB}(C) \rangle - \langle I_{dB}(N) \rangle \quad (32)$$



(a) Filter: frequency spectrum and phase response

(b) Image after AM with filter

Figure 14: Filter used in amplitude modulation. Filter length 25, filter is smoothed.

TS is a measurement for the amount of suppression of signal from tissue when a modulation technique is applied to the echoes. This is done by comparing the intensity in the modulated tissue signal, T2, to the unmodulated tissue signal, T1:

$$TS_{dB} = \langle I_{dB}(T1) \rangle - \langle I_{dB}(T2) \rangle \quad (33)$$

## 5 Results

A presentation of the most important and illustrative results attained from the measurements and post processing of data are presented in this chapter. This includes measurements of the transmitted pulses, the performances of different AM filters and demonstrations of the reverberation problem in AM.

### 5.1 Transmitted pulses with different amplitude

Figure 15 and 16 shows the measured electrical and acoustical pulses in both time and frequency domain. The frequency plots are limited between 0.5 MHz and 4.5 MHz, which covers the pass-band of the probe used in the experiments, and they are normalized in order to observe their symmetrical properties. The pulses specified on the scanner are squared with 5 half periods, center frequency at 1.5 MHz and the power levels employed are 2.5V, 5V and 10V. The electrical pulses are measured on the FEC as described in 3.1, while the acoustical pulses are recorded using a hydrophone in the near field (5 mm from the probe), section 3.2.

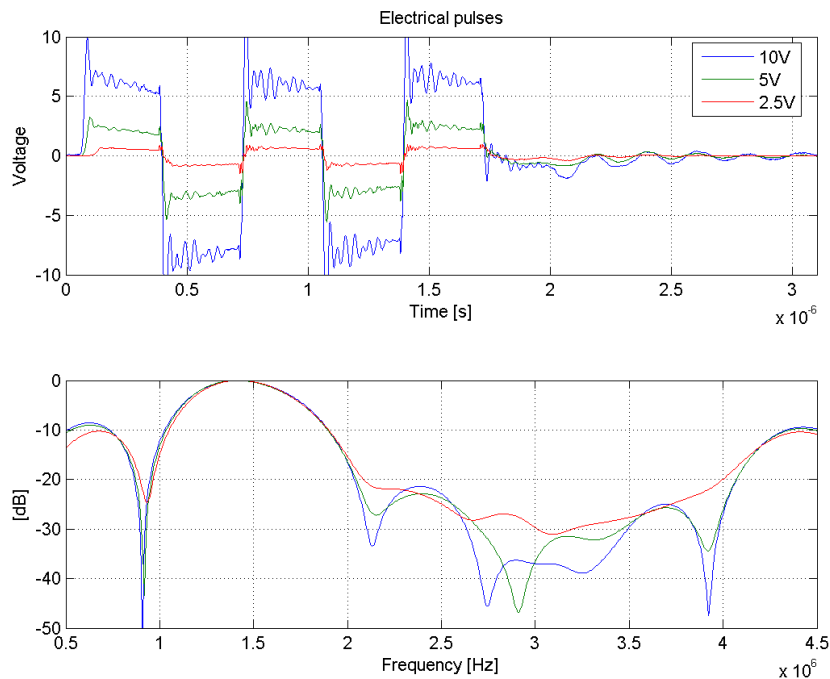


Figure 15: *Electrical pulses*

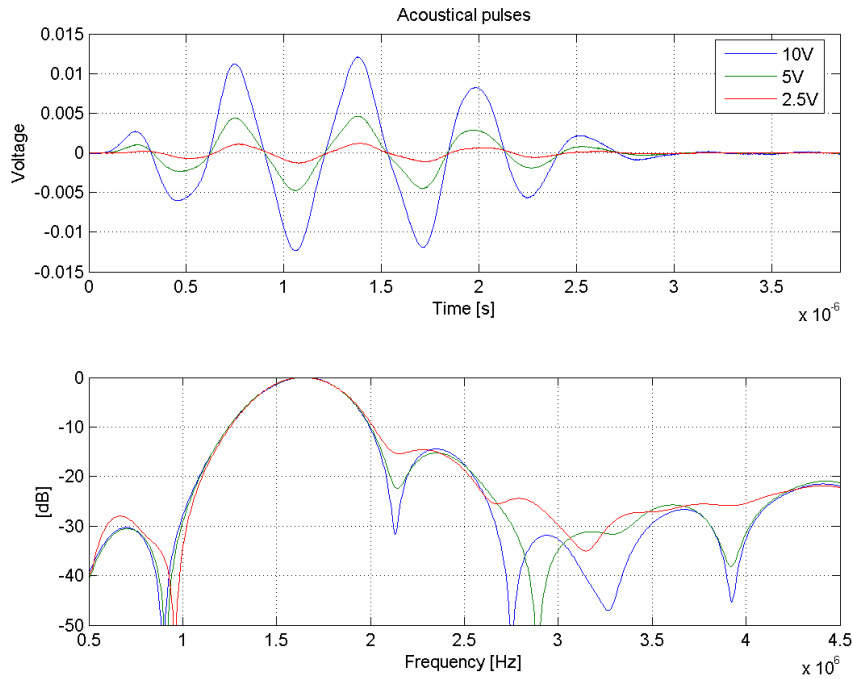


Figure 16: *Acoustical pulses. Scaling: 12.2 MPa/V*

The first observation made is that the electrical measured pulses do not agree with the voltage level specified on the scanner. A specification of 10V gives about 6.2V (positive) and 8.3V (negative), 5V gives +2.2V and -3.3V, and 2.5V gives +0.5V and -0.8V. The error seems to be greater (in percentages) for lower power levels. The second observation is from the normalized frequency plot which reveals a dissymmetry between the pulses outside the centre frequency. This can also be seen from the acoustical pulses.

## 5.2 Suppression by AM

Figure 17 and 18 contain frequency plots of the electrical and acoustical pulses where two pulses with different amplitude are subtracted after the lower one has been adjusted with an optimal constant to get a maximal suppression (AM). The pots also include pulse inversion (PI), where two pulses with opposite polarity are added. The results are normalized to the maximum value of the higher pulse to illustrate the suppression. The AM plots for the electrical pulses include both the situation where the same HV-power supply and two different HV-power supplies are used to generate two pulses with different power.



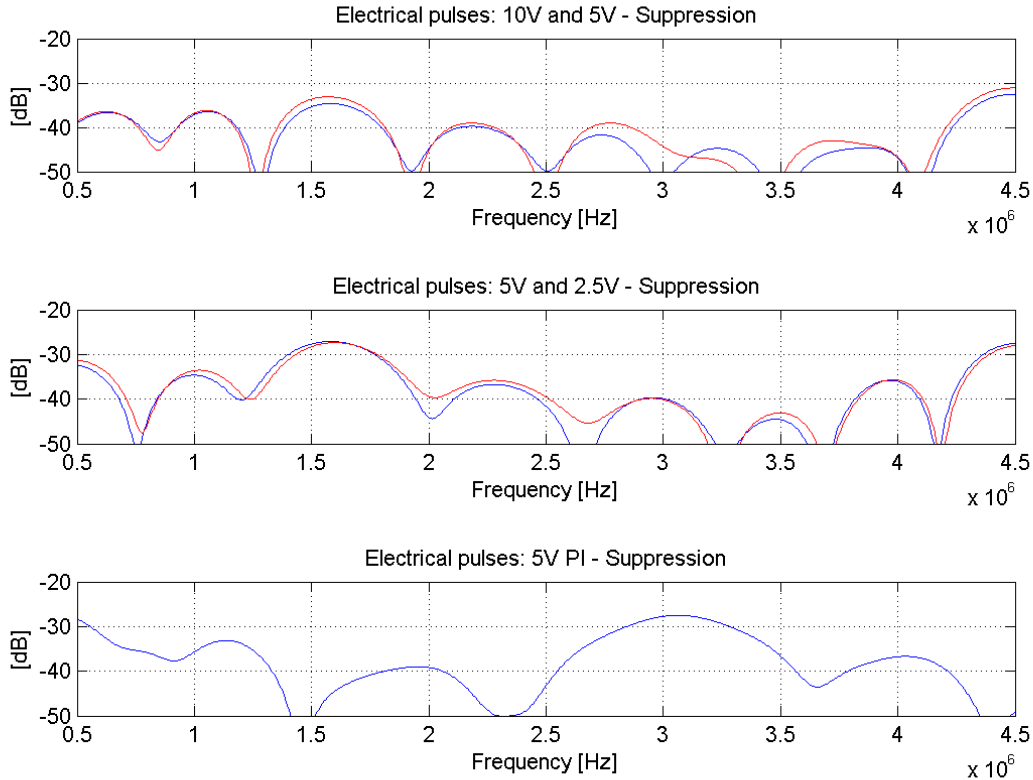
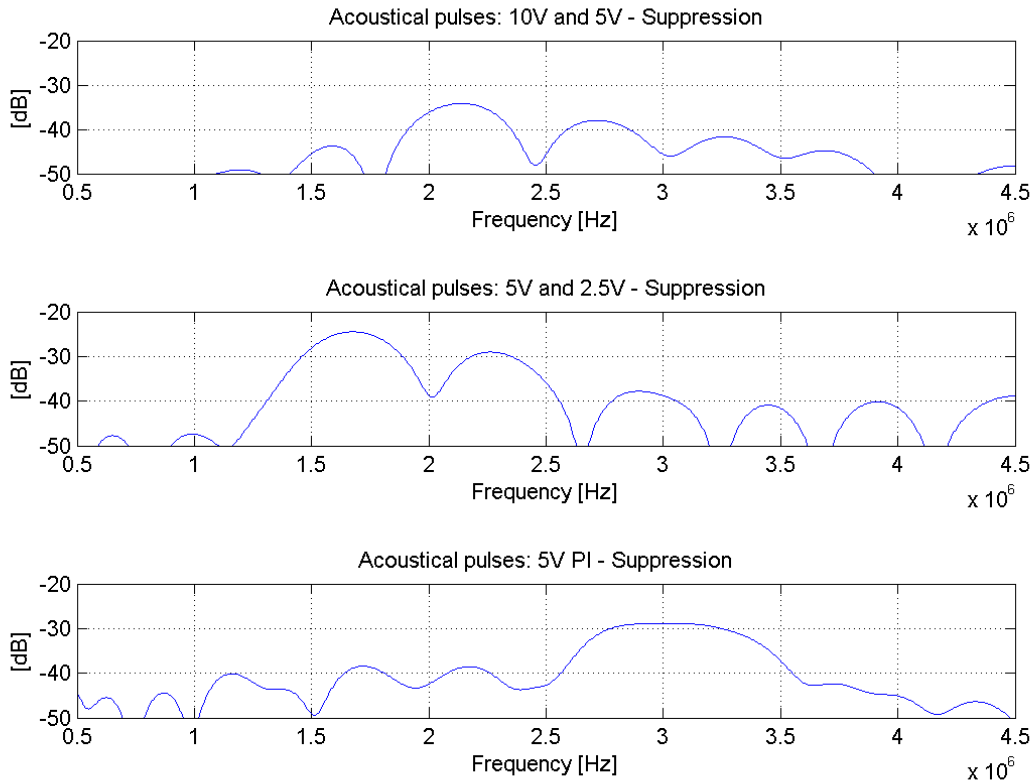


Figure 17: *Electrical pulses.* The *blue graph* shows the suppression attained by AM when the same HV-power supply is used for both pulses, while the *red graph* illustrates the suppression when two different HV-power supplies are employed.

The same procedure is done on the received echoes from the tissue phantom, using the same pulses. This can be seen in figure 19.

From figure 17 and 18 it seems like the acoustical and electrical pulses achieves the same level of suppression after AM. The 5V and 10V pulses gives about 5-10 dB better suppression compared to 2.5V and 5V pulses. The use of different HV-power supplies does not seem to affect the level of suppression considerably for the electrical pulses. When AM is applied on echo data does the suppression level drop about 5-10 dB, compared to the electrical and acoustical pulses, see figure 19. PI attains better suppression at the center frequency, compared to AM. But outside the fundamental frequency (e.g. 2nd harmonic) is AM superior to PI.

Figure 18: *Suppression by AM of acoustical pulses*

### 5.3 Reverberations

As described in 3.3.2 did a problem occur when pulse number 1 and 3 from the pulse packet given in (15) were used in AM. The tissue signal was not suppressed as well as desired. To investigate this further were four pulse packets, given in (16)-(19), used to acquire data from the flow phantom. The intention with this experiment was to reveal whether reverberations caused the problem, and also to study how adding different reverberation pulses affected the images after amplitude modulation. In figure 20 the images from the four pulse packets can be viewed. In AMi, in the upper right corner, is no reverberation pulses added, and a strong signal can be observed on the left hand side of the image. In AMii a reverberation pulse has been added in such a way that both pulses used to create the image have an equal pulse in front. Here the signal is reduced, yet it still is quite significant. In AMiii two pulses have been added, so the pulses used in the imaging have a relatively equal pulse in front. The signal in the two other AM images is absent here.

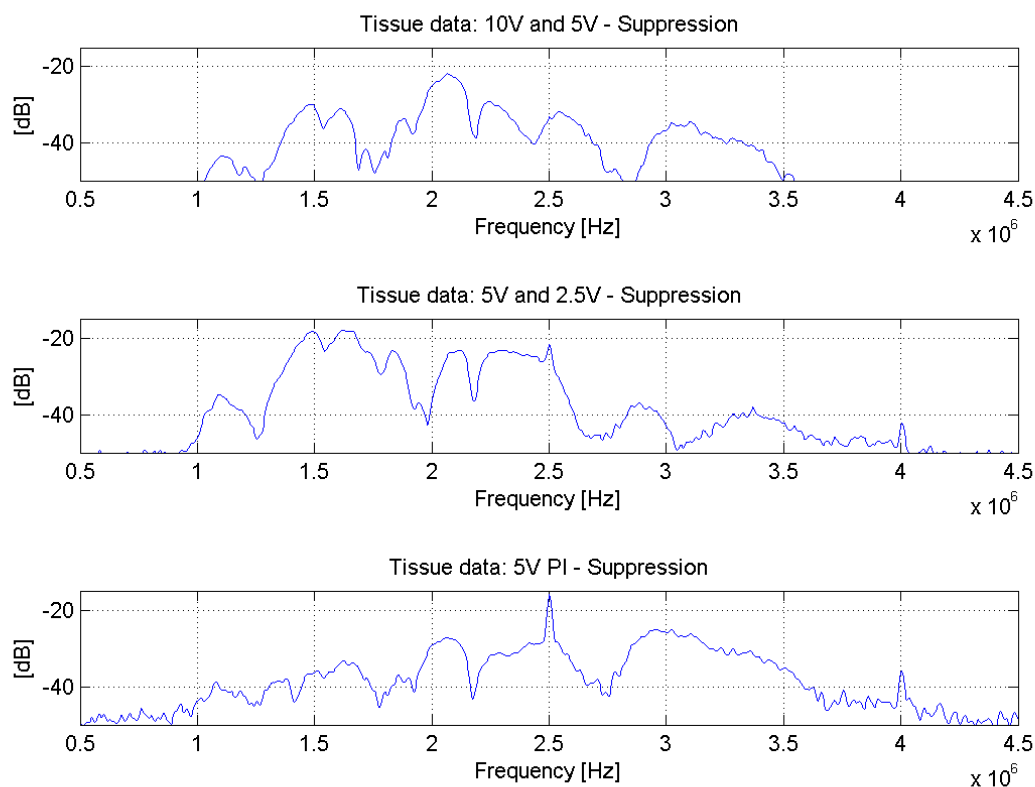


Figure 19: *Echo-data from the tissue phantom suppressed by AM*

In the upper left corner of the figure has a packet of two pulses with opposite polarity been transmitted to create a PI image, the echo signals have been  $2^{nd}$  harmonic filtered. As in AMiii is the strong signal not present here.

In figure 21 are the frequency spectra of a tissue area (see section 4.2) from all images in figure 20 plotted. The observations made from the grayscale images are clearly supported by the spectra. AMi and AMii have a strong fundamental signal in the tissue area, compared to AMiii. PI has no fundamental signal due to the filter. Also notice the stronger  $2^{nd}$  harmonic signal in PI compared to AM.

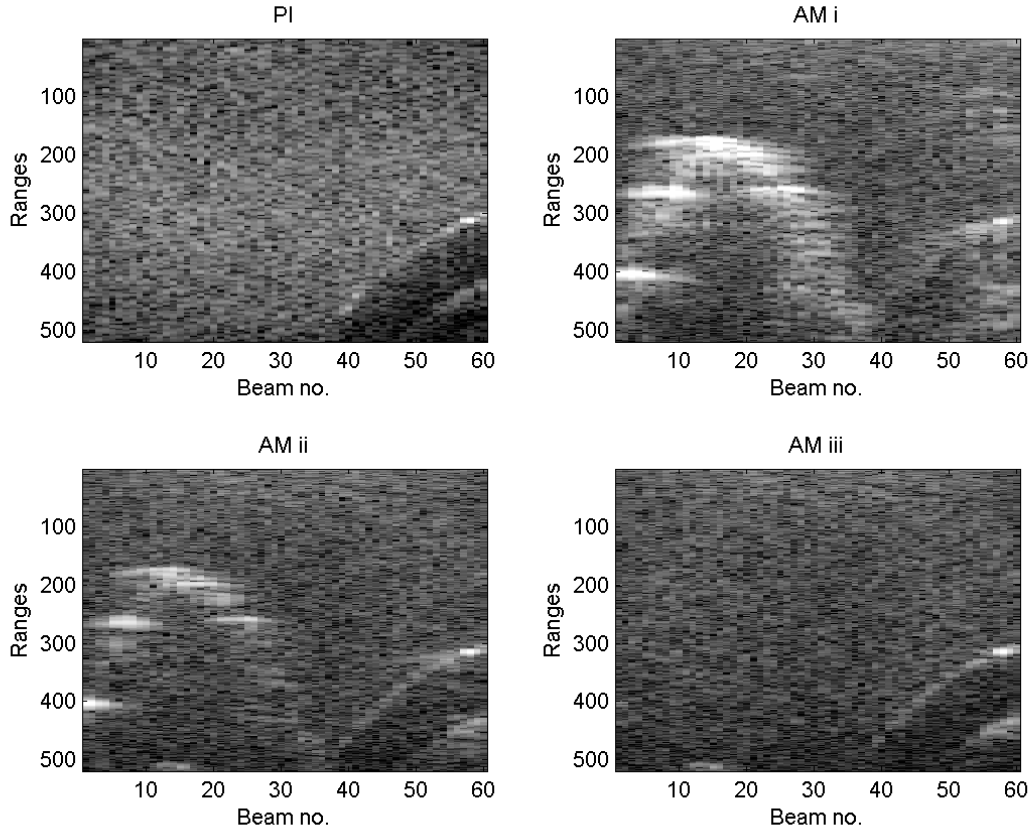


Figure 20: Reverberations in amplitude modulation.  $PI: [-\underline{1} \ \underline{1}]$  ( $2^{nd}$  harmonic filtered),  $AMi: [\underline{\alpha} \ \underline{1}]$ ,  $AMii: [\alpha \ \underline{\alpha} \ \underline{1}]$ ,  $AMiii: [\alpha \ \underline{\alpha} \ \underline{1} \ \underline{1}]$ . The pulses underlined are the ones used in the imaging, the others are added as reverberation pulses.

## 5.4 AM filters

### 5.4.1 Filter from electrical and acoustical pulses

Figure 23 shows the spectrum plots of the tissue signal after AM. The echoes are acquired from the tissue phantom. The figure illustrates the difference in tissue suppression when a constant factor ( $\alpha$ ) is used for AM compared to the use of a filter computed from the electrical or acoustical pulses. The different filters are presented in figure 22. Table 6 summarizes the tissue suppression for all three methods. Here it is revealed that the neither the electrical nor the acoustical filter does outperform a constant factor.

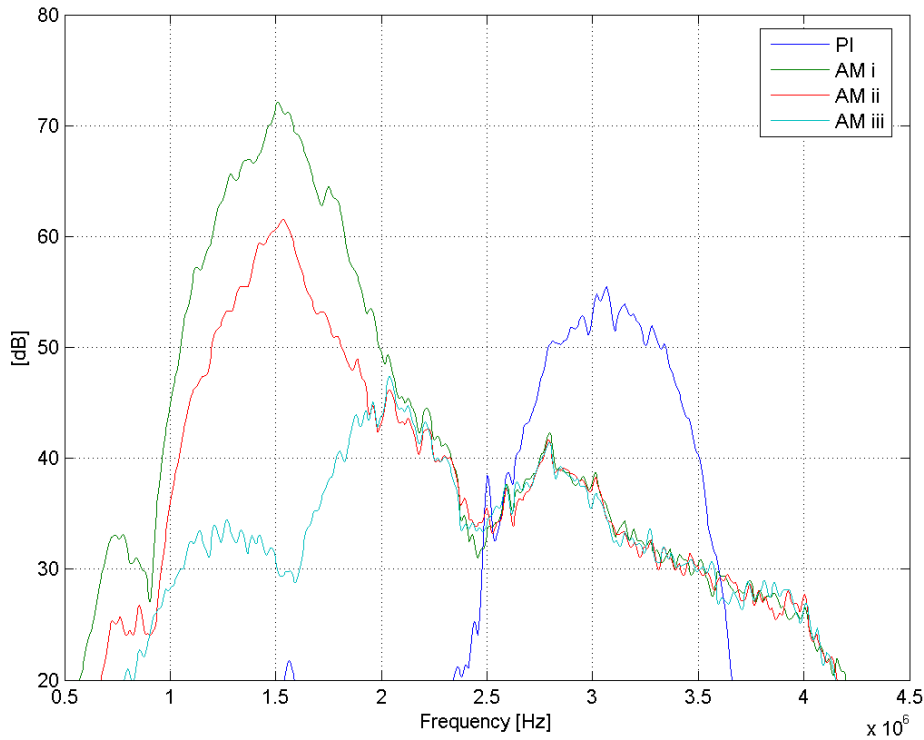


Figure 21: *Frequency specter of a tissue area from the images in figure 20.*

#### 5.4.2 Filter from tissue data

As described in section 4.4.3 a filter from echo data was the third attempt to make a filter which outperformed the constant downscaling factor in AM. In figure 24 is an example shown for a filter to be used in AM. The filter is made from a tissue phantom, and is tested out on a flow phantom. The transmitted pulses used in this case are at 5V and 3.79V. The magnitude and phase response of the filter are illustrated in 24a. The constant factor is traced with a red line to be compared to the filter.

The grayscale images in figure 25 compares the use of a constant factor to the filter. In these images it seems like the filter does perform a better suppression of tissue, but the suppression is not completely to the noise level (which is the lowest achievable tissue level). A more particular illustration of the signal strength from tissue and contrast is demonstrated in figure 24b, where the spectra of an area containing contrast agent and a pure tissue area are plotted. The dotted lines shows the level when the filter is applied, whereas the solid lines indicates the result of the constant factor.

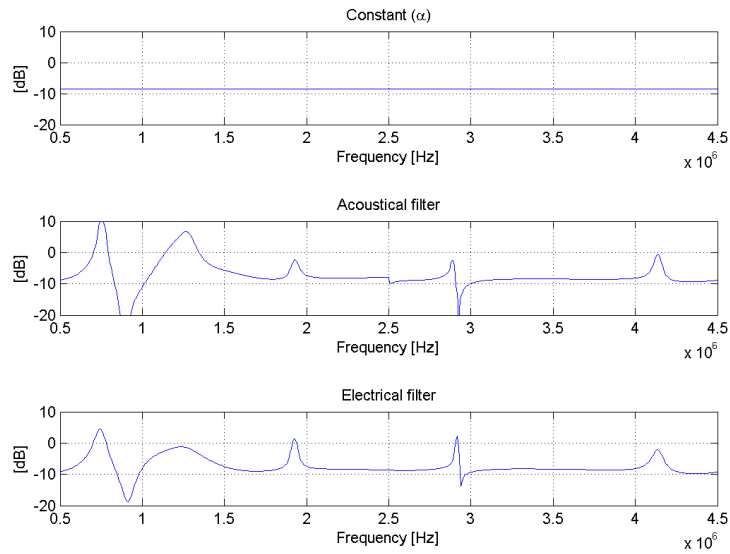


Figure 22: *Constant, electrical and acoustical AM filters. 5V and 10V transmitted pulses.*

Table 6: *Tissue suppressed by AM for different filters [dB]*

Transmitted pulses	Constant ( $\alpha$ )	Electrical filter	Acoustical filter
5V and 10V	17.8	16.4	16.2

The AM filter for 7/5V pulses and the same results as for 5/3.79V can be found in figure 26 and 27. And also the results obtained for 10/6.84V pulses are shown in figure 28 and 29. Observe how the tissue signal becomes stronger as the power of the transmitted pulses increases.

In figure 30 and 31 are the tissue suppression attained for AM, PIAM and PI quantified, including both 2.5 and 3.5 periods transmitted pulses. AM provides better suppression than PI and PIAM, and the filter does improve TS with 1-3 dB for AM and PIAM. Also notice how TS increases slightly as the transmitted power increases for AM, while it decreases for PI.

In figure 32 and 33 are the CTR and CNR calculated for the case where Optison is used as contrast agent. The filter does also increase CTR, although a little less (about 0.5 dB) compared to TS. However this is not enough for AM or PIAM to do better than PI for 5/3.79V transmitted pulses. From figure 33 it seems like the filter decreases the CNR by 0.5 dB. Furthermore observe how PI provides the best CNR.

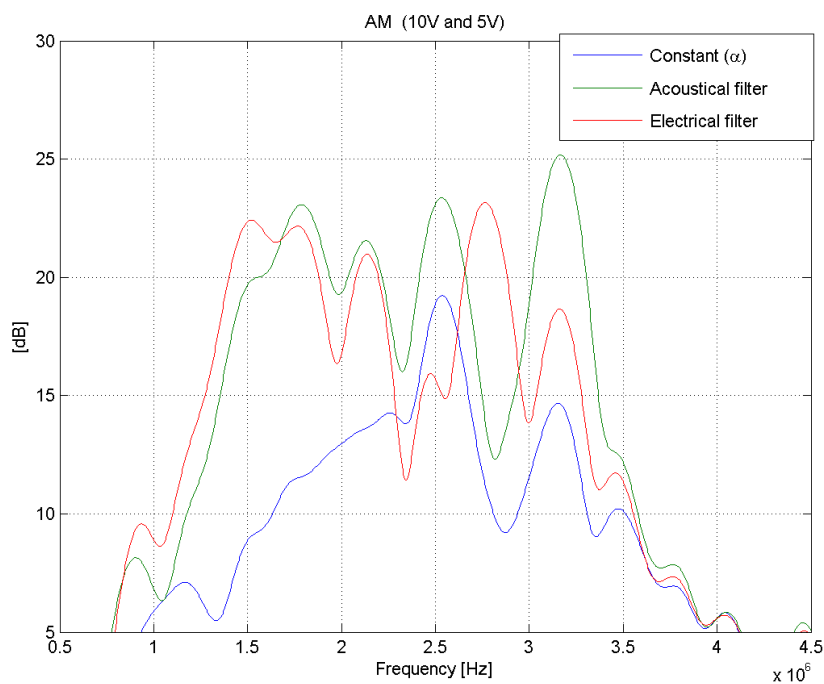
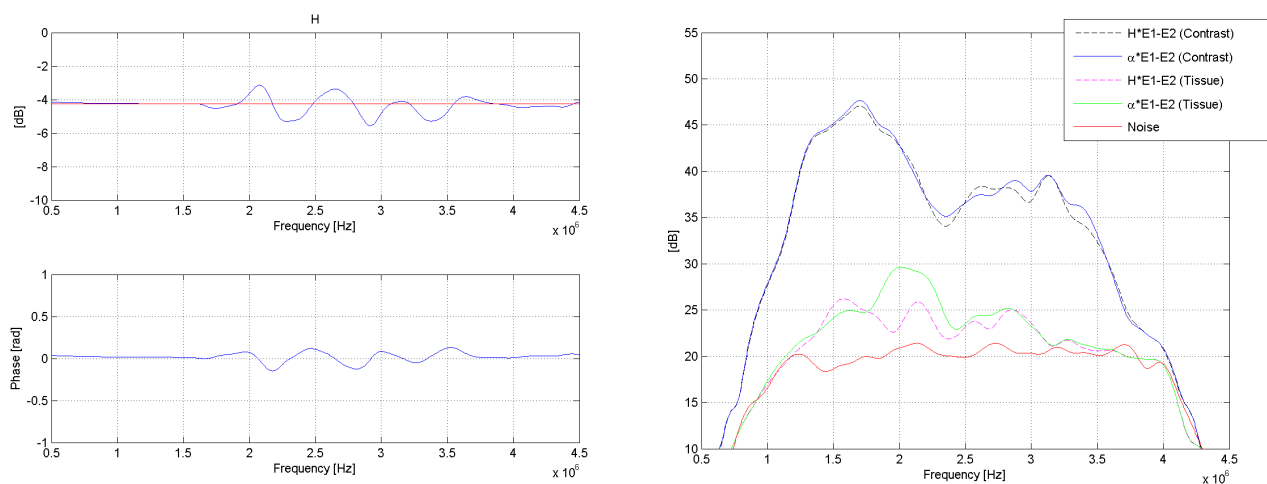


Figure 23: *Tissue suppressed by AM with a constant, electrical filter and acoustical filter. 5V and 10V pulses are transmitted.*

Results of the same experiment, only with Sonazoid instead of Optison, can be found in figure 34 and 35. There are no large variances by the substitution of contrast agent. The filter does still provide better CTR, while CNR is slightly decreased. But PI does afford the best result for the lower voltage.

This experiment was also done with pulses of 3.5 periods. Tables of all results can be found in appendix A.



(a) Filter magnitude and phase response      (b) Spectra from contrast area and tissue area

Figure 24: Filter from phantom data: AM, 2.5 periods transmitted pulses at 5/3.79V, contrast agent: Optison. Comparing a constant upscaling factor ( $\alpha$ ) with a filter in AM.

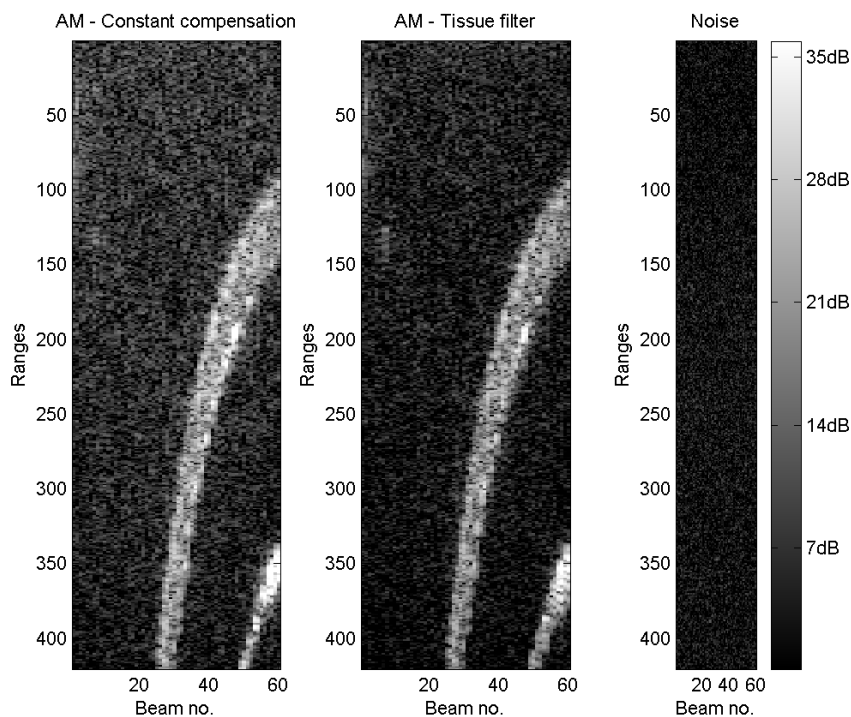
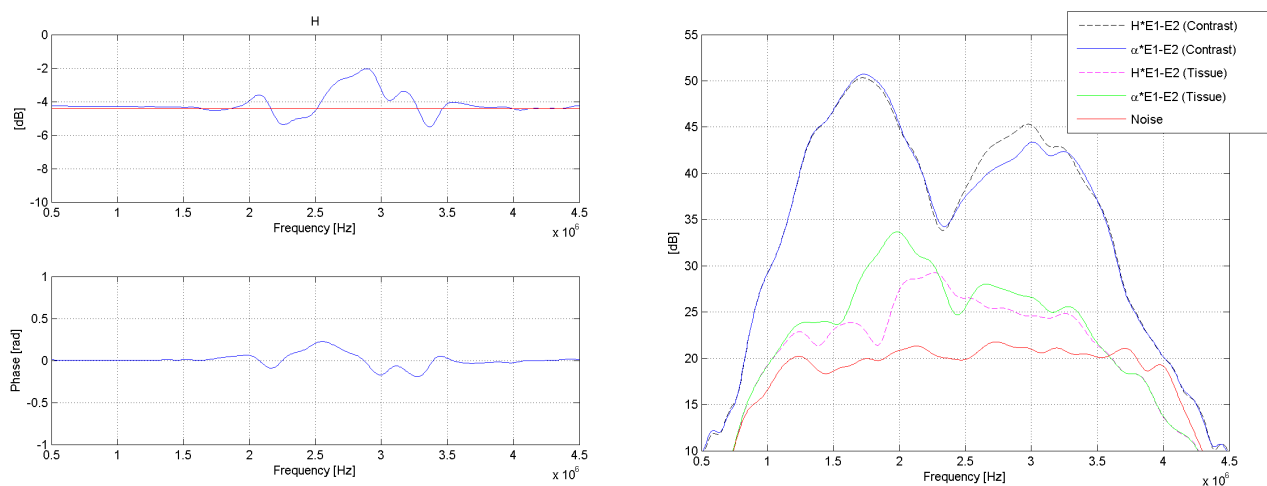


Figure 25: Grayscale images from the flow phantom. AM, 2.5 periods transmitted pulses at 5/3.79V, contrast agent: Optison. Gain: -5dB, dynamic area: 35dB.





(a) Filter magnitude and phase response      (b) Spectra from contrast area and tissue area

Figure 26: Filter from phantom data: AM, 2.5 periods transmitted pulses at 7/5V, contrast agent: Optison. Comparing a constant upscaling factor ( $\alpha$ ) with a filter in AM.

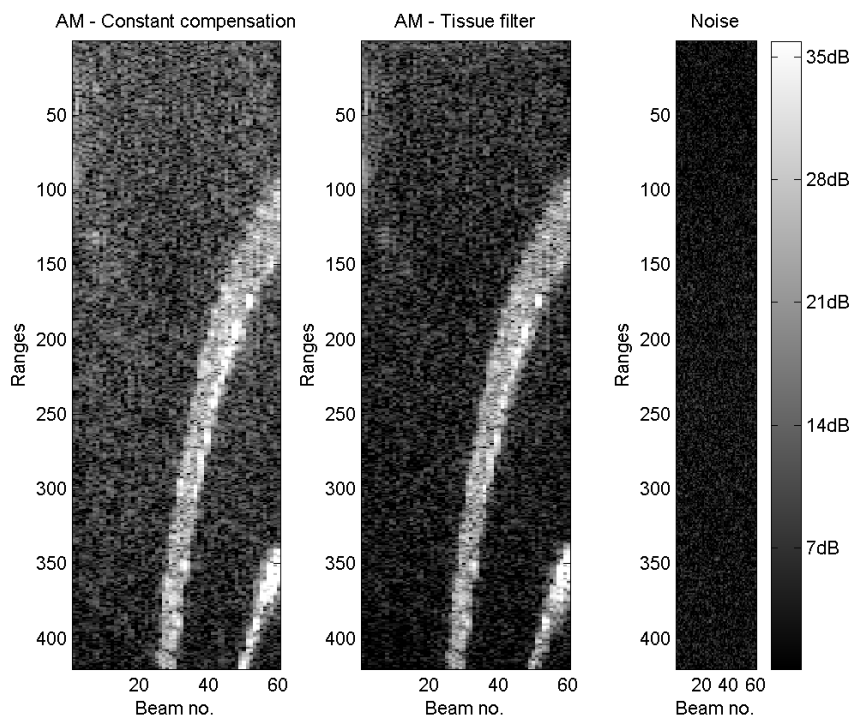
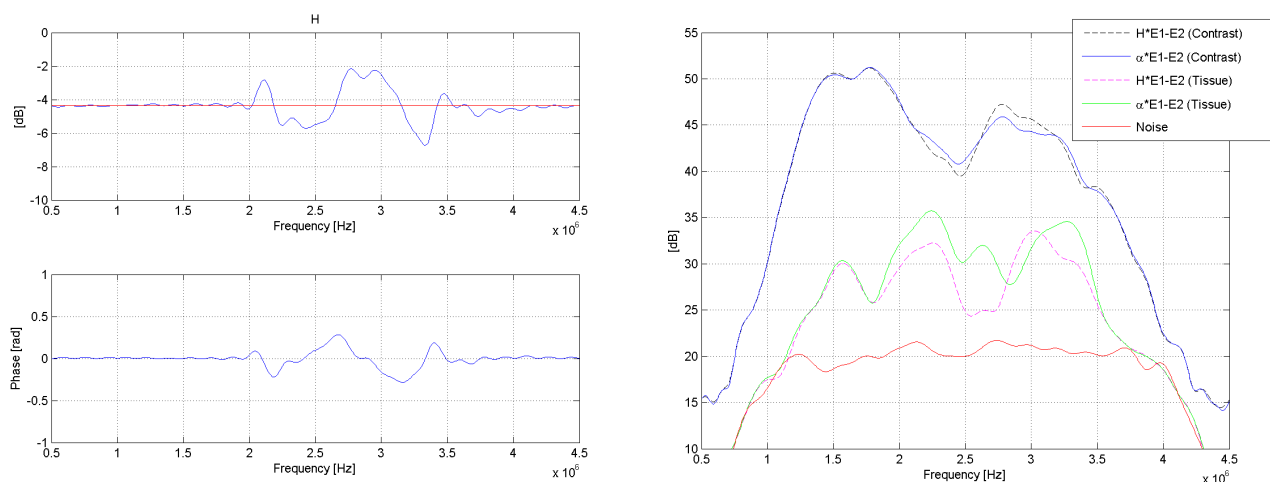


Figure 27: Grayscale images from the flow phantom. AM, 2.5 periods transmitted pulses at 7/5V, contrast agent: Optison. Gain: -5dB, dynamic area: 35dB.



(a) Filter magnitude and phase response (b) Spectra from contrast area and tissue area

Figure 28: Filter from phantom data: AM, 2.5 periods transmitted pulses at 10/6.84V, contrast agent: Optison. Comparing a constant upscaling factor ( $\alpha$ ) with a filter in AM.

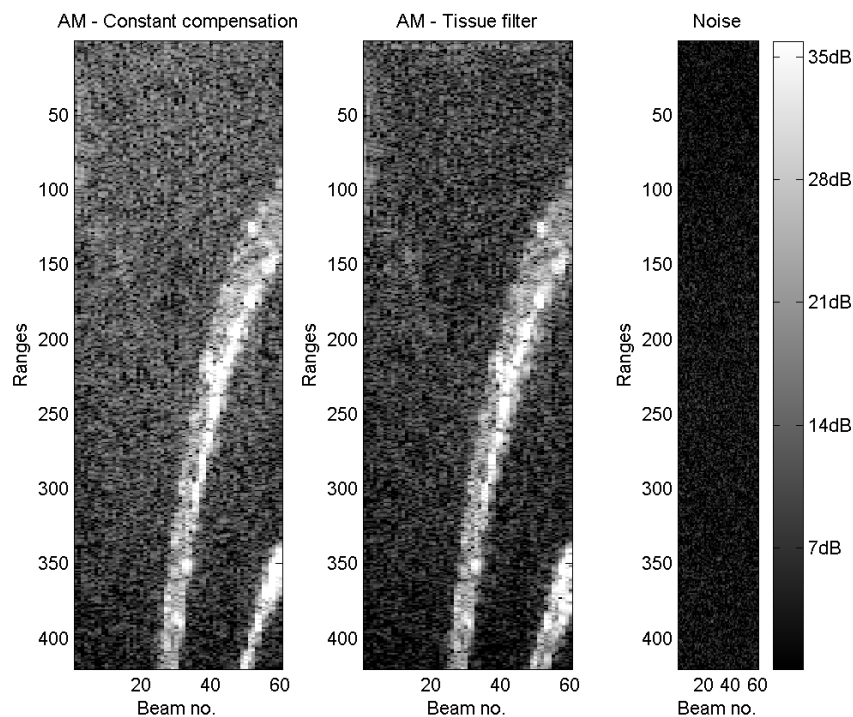


Figure 29: Grayscale images from the flow phantom. AM, 2.5 periods transmitted pulses at 10/6.84V, contrast agent: Optison. Gain: -5dB, dynamic area: 35dB.

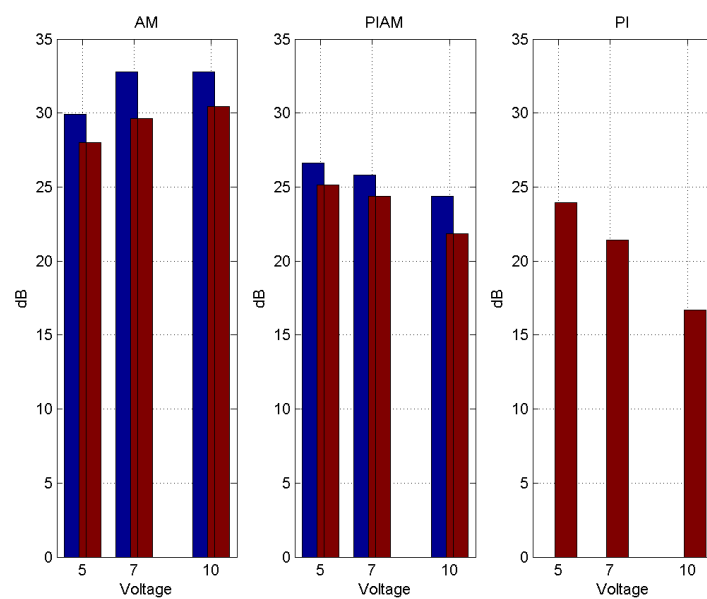


Figure 30: Tissue Suppression for 2.5 periods pulses. The red bars are the TS level when a constant is used, the blue when a filter is used.

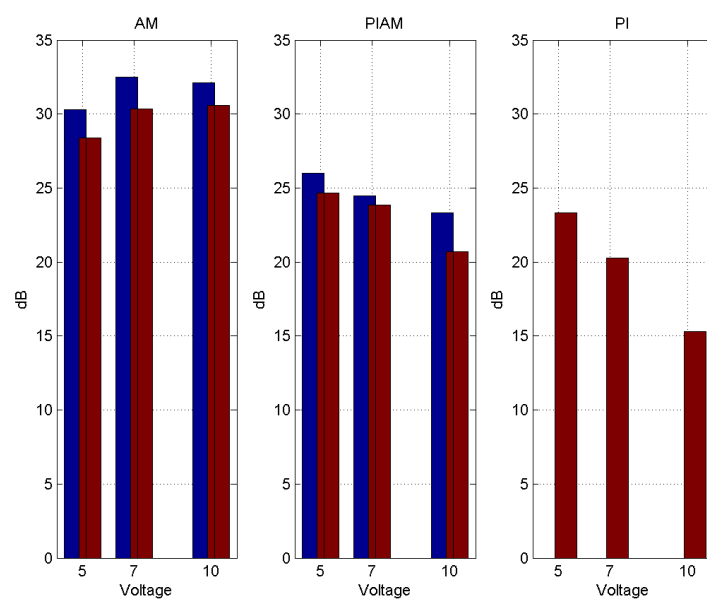


Figure 31: Tissue Suppression for 3.5 periods pulses. The red bars are the TS level when a constant is used, the blue when a filter is used.

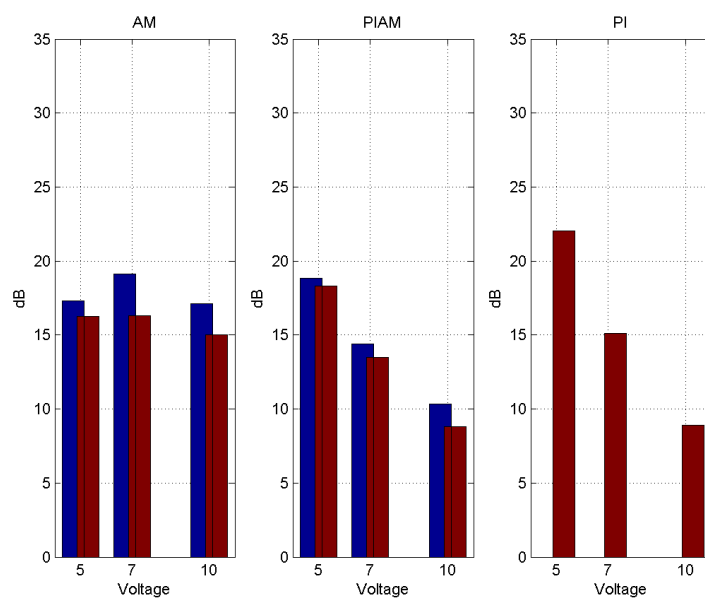


Figure 32: Contrast-to-Tissue-Ratio for 2.5 periods pulses and Optison contrast agent. The red bars are the TS level when a constant is used, the blue when a filter is used.

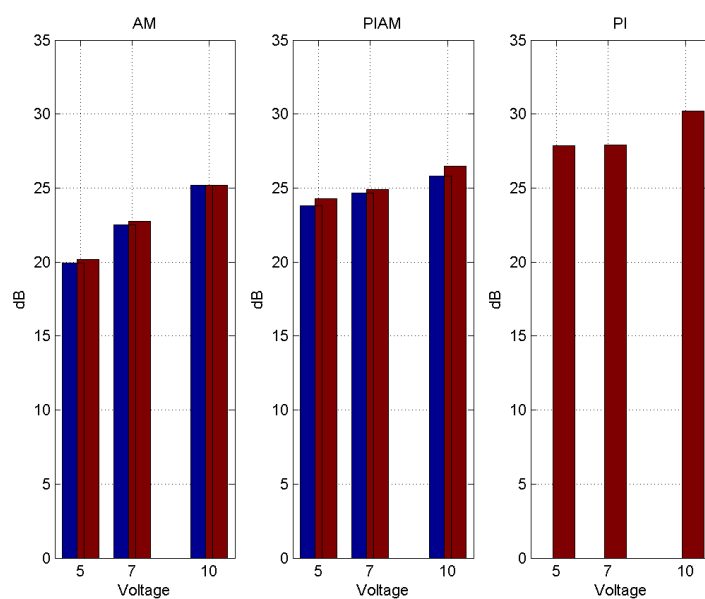


Figure 33: Contrast-to-Noise-Ratio for 2.5 periods pulses and Optison contrast agent. The red bars are the TS level when a constant is used, the blue when a filter is used.

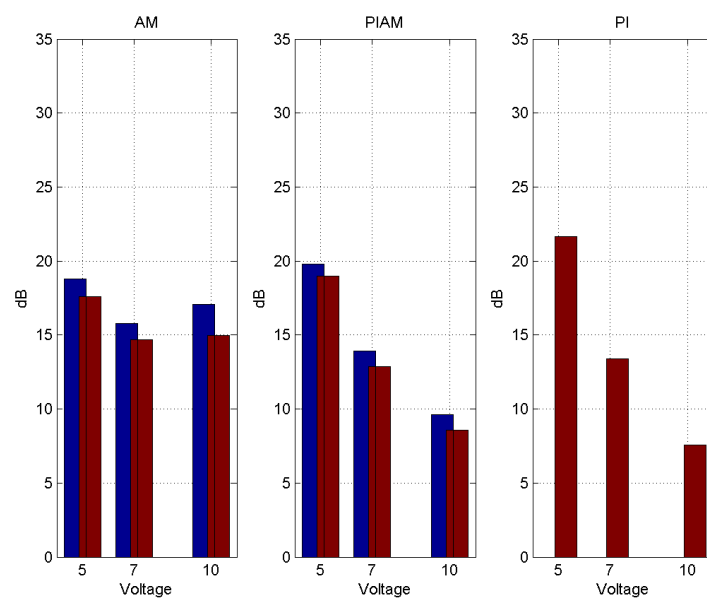


Figure 34: Contrast-to-Tissue-Ratio for 2.5 periods pulses and Sonazoid contrast agent. The red bars are the TS level when a constant is used, the blue when a filter is used.

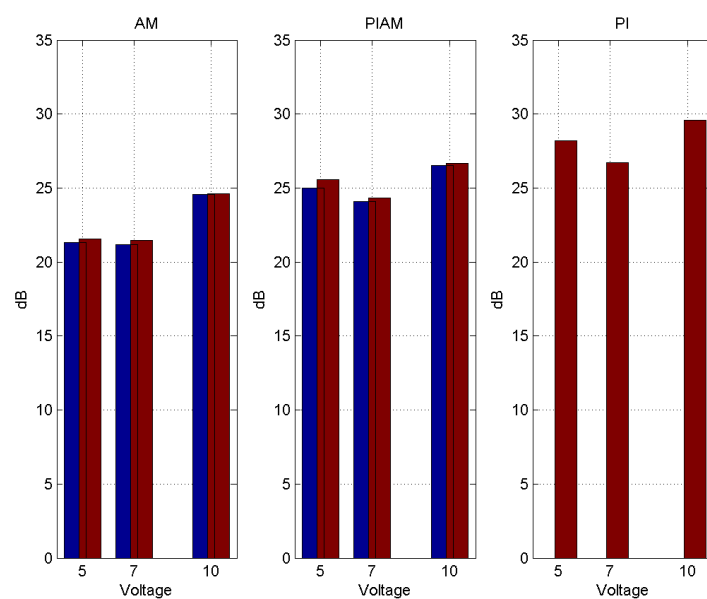


Figure 35: Contrast-to-Noise-Ratio for 2.5 periods pulses and Sonazoid contrast agent. The red bars are the TS level when a constant is used, the blue when a filter is used.

## 6 Discussion

### 6.1 Choice of settings

The electrical and acoustical pulses were measured at an early stage in the diploma work. At that time were pulses with power 2.5, 5 and 10 V tested out. Because the scanner did not provide the exact voltage specified was the AM-factor ( $\alpha$ ) fairly high, about 19 dB between 10 and 5 V pulses, and about 29 dB between 10 and 5 V pulses. Consequently the pulses employed in the later experiments were adjusted to have a smaller power distance among them.

All measurements have transmitted pulses at 1.5 MHz, in order to have both the fundamental and 2<sup>nd</sup> harmonic frequency component of the echo signal in the pass-band of the probe. Furthermore were both pulses with 2.5 and 3.5 periods tested out, to see if the pulse length affected the contrast signal, and observe differences in tissue suppression both with and without the developed AM filter.

### 6.2 Transmitted pulses

As mentioned above, the transmitted electrical pulses did not have the exact power level as specified on the scanner. This is not a serious problem for the use of amplitude modulation, because it is uncomplicated to find an appropriate value from i.e. the echo signal, and use this to downscale the echoes from the high-powered pulse. Furthermore the frequency spectra of both the electrical and acoustical pulses indicate a dissymmetry between pulses with different amplitude. Therefore no matter how good the constant factor we might calculate is, it will not be able to suppress linear signal in the entire pass-band of the probe. In order to compensate for the dissymmetry between the two transmitted pulses were several attempts made to creating a filter which intention was to replace the constant factor, and thus increase the suppression of linear signal.

#### 6.2.1 Two HV-power supplies

When amplitude modulation is employed the scanner applies two different HV-power supplies to generate two pulses of different voltage. The use of two supplies was considered to be a possible source of the asymmetry between pulses of different amplitude. In figure 17 are a comparison made of the suppression achieved in the electrical pulses when both a single and two HV-power supplies were employed to create two pulses of different amplitude. As the plots illustrate, there is no considerable difference in the suppression, which excludes this to be a source of the pulse asymmetry.

### 6.3 Reverberation problem in AM

The results in the project work by the author [12] did suffer from low TS around the transmitted frequency. This was particularly a problem when low frequency pulses were transmitted, around 1.5 MHz, but not a significant problem when the pulses were transmitted at 2.5 MHz. The lack of tissue suppression was closely discussed in the project, and the most supported assumption was a phase shift or dissymmetry between the transmitted pulses of different amplitude. But from the results of the investigation of the electrical and acoustical pulses, which can be found in 5.1, are the pulses clearly symmetrical around the transmitted frequency. The dissymmetry occurs mainly in the upper part of the frequency band. Thus, the assumption made in the project is most likely incorrect.

The same problem occurred in the diploma work too. But by substituting the two pulses used in AM to two other pulses from the pulse packet seemed to eliminate the problem. This led to a new hypothesis of the source of the error; reverberations. In order to look more closely into the phenomenon a measurement with three transmitted pulses was performed, where the first was added as a reverberation pulse in such a way that the two pulses used in the imaging did have an equal pulse in front. This did reduce the strong tissue signal at the fundamental frequency about 10 dB, but the signal could still be seen in the grayscale images, see section 5.3. So, to improve the suppression even further another experiment was carried out, this time with four pulses in the packet so both pulses utilized for the imaging now had a relatively equal pulse in front. And as figure 20 and 21 demonstrates does this eliminate the problem more or less completely.

The results of this experiment demonstrate the problem with reverberations in amplitude modulation clearly. To get rid of reverberations do not only the pulses employed in the imaging process need to summarize to zero after downscaling, the pulses in front of each pulse used need to summarize to zero as well. As can be seen in figure 20 are reverberations no problem in PI, as long as the fundamental frequency component is removed by a band-pass filter. But why were not the reverberations notable in [12] when transmitting 2.5 MHz pulses? It might be reasoned by the higher attenuation caused by higher frequency.

In the project work [12] the tissue suppression attained when transmitting 2.5 period pulses of 4.37/3.26 V at 1.5 MHz was 12.6 dB in AM. No experiment has been performed with such low power here, but an assessment with 5/3.79 V pulses demonstrates remarkable results. As can be seen from figure 30 is the TS 28.0 dB in AM (without the AM filter, see the following subsection). The bar charts indicates an increase of TS as the pulse voltage increases in AM, so the comparison is not totally fair, but an assertion of at least 13 dB gain is most likely maintainable. In the bar chart only an increase of 2 dB TS can be found from 5/3.79 V to 7/5 V pulses, this supports the assertion of at least 13 dB gain.

Because of strong reflections from the bottom of the flow phantom and from the pipeline inside the phantom, reverberations are extraordinarily significant. It is worth noticing that reverberations probably will not be as strong in the imaging of human tissue, but might be a problem close to bone structures as the ribs in cardiography.

## 6.4 Filter vs. constant in AM

Several attempts to make a filter to replace the constant AM factor were performed. Filters created from electrical and acoustical pulses were tested out, before a filter based on echoes from a phantom was found to be superior.

### 6.4.1 Filter from electrical and acoustical pulses

Neither the filter from the electrical pulses nor the filter based on acoustical pulses did increase the tissue suppression when tested out on echo data from a tissue phantom. Surprisingly did the filtering process result in about 1.5 dB poorer suppression (see table 6). From figure 23 it seem like both filters provide an inferior suppression around the transmitted frequency (1.5 MHz) compared to the constant factor. This might be due to the dissymmetry in the pulses around 0.9 MHz (figure 15 and 16). When the filters make a correction of this error, the fluctuation around 0.9 MHz is smeared out in the frequency domain, resound by the limited filter length, which causes a poorer suppression, see figure 22.

### 6.4.2 Filter from tissue data

Figure 17-19 shows the electrical pulses, acoustical pulses and tissue data after amplitude modulation using a constant downscaling factor. The plots indicate a 5-10 dB drop of suppression from electrical and acoustical pulses to tissue echoes. This reduction is most likely due to nonlinear propagation in the tissue phantom. In combination with the non-successful use of filter from electrical and acoustical pulses, this observation lead to the idea of testing out a filter created of echo data from the phantom. To make it as realistic as possible the filter had to be tested on data from another phantom, which was carried out by the use of the filter on a flow phantom containing contrast agent. Thus would the result of the filtering process not only indicate the amount of tissue suppression, but also the affect the filter had on the contrast signal.

Figure 24-29 illustrates how the filters have an effect on the amplitude modulated echoes. You can clearly see from the spectra plots that the filters provide better tissue suppression in the frequency area around 2.2 MHz. If you go back to figure 15 and 16, a dissymmetry



in the transmitted pulses can be found at this frequency. So, the successful filtering around this frequency is probably due to the correction of the pulse dissymmetry and not a result of similar nonlinear propagation in the two phantoms. Also notice from the filter spectra how the filters are constant, approximately at the  $\alpha$ -value, in the lower part of the frequency band. Remember how the electrical and acoustical filters performed compensation in this frequency area, which corrupted the filter. The dissymmetry below 1 MHz in the transmitted pulses does thus not affect the echoes because of the low level (about 30 dB below the maximum in the acoustical pulses). Therefore, when the acoustical or electrical filter makes a correction in this region, will it mainly result in noise being filtered which enhances the noise signal and diminishes the suppression.

Accordingly does the AM filter enhance TS, this is illustrated in figure 30 and 31, where both TS with and without filter is shown in a bar chart. The TS improvement in AM, which is summarized in table 7, is 1.5-3.2 dB. As can be observed in the table is the increase in CTR 0-1.4 dB lower compared to TS, which implies a small decrease of contrast signal when filtering is applied. As a consequence of the contrast signal drop is the CNR reduced by 0-0.6 dB when filtered, compared to the use of a constant factor. The drop in the intensity of the contrast signal is probably due to nonlinearities from the transmitted pulses being removed, in the same manner as, but fortunately not as much as the more linear tissue signal.

Table 7: AM: Improved TS, CTR and CNR with AM filter (Optison contrast agent) [dB]

	2.5 periods			3.5 periods		
	5/3.79V	7/5V	10/6.84V	5/3.79V	7/5V	10/6.84V
TS	1.9	3.2	2.4	1.9	2.2	1.5
CTR	1.0	2.8	2.1	1.3	1.4	1.5
CNR	-0.3	-0.3	0.0	-0.4	-0.6	-0.5

### PIAM vs. AM

Also when pulse inversion is included to AM, i.e. PIAM, does the filtering process provide better tissue suppression, according to figure 30 and 31. But the gain is slightly lower for PIAM, in average 1.7 dB compared to 2.2 dB for AM. Also the gain in CTR is higher for AM; 1.7 vs. 1.0 dB.

### Pulse length

The AM filter seems to have a higher effect on data from pulses of 2.5 periods compared to 3.5 period pulses. The TS has a mean value of 2.2 dB for 2.5 p and 1.7 dB for 3.5 p, while CTR is 1.7 dB for 2.5 p and 1.0 dB for 3.5 p.

## 6.5 Which modulation technique is best?

The experiments carried out are mainly performed with a view to develop and observe the performance of the AM filter. But also a comparison between the different modulation techniques has been made, see figure 30-35. As can be observed PI provides the best CTR even as a full-band technique<sup>1</sup> at the lowest voltage level. The reason why PI is better than PIAM is probably the higher average transmitted power in PI, which furthermore produces a stronger 2<sup>nd</sup> harmonic component<sup>2</sup>. To have the same average power in the two methods was PI with 6.08V pulses tried out to be compared with AM 7V and 5V pulses. But because of a higher amount of bubble destruction at higher powers and unstable concentration of contrast agent was this assessment not successful. The problem with unstable contrast concentration makes it hard to make any comparison of CTR and CNR between different transmitted powers, different pulse lengths and the two contrast agents. However what can be assessed are the different modulation techniques within each measurement, which are from the same pulse packet. TS for all settings can obviously also be assessed as it is not dependent on the contrast signal.

At transmitted power of 7/5V and 10/6.84V does AM have a superior CTR to both PI and PIAM. This is a strange result as PIAM always has a higher contrast level than AM<sup>2</sup>, thus must the explanation be the higher amount of tissue signal in the 2<sup>nd</sup> harmonic, caused by nonlinear propagation. The assumption is supported by the lower TS in PI and PIAM compared to AM. Also notice how TS increases with higher power in AM, while it decreases in PI and PIAM, which demonstrates the problem of nonlinear tissue signal when high powered pulses with opposite polarity are transmitted.

At the lowest voltage level, 5/3.79 V, does PI provide the best CTR. But it is uncertain if this is a fair assessment as PI has a higher average transmitted power compared to AM and PIAM. The uncertainty is if the amount of bubble destruction is associated with the most powerful transmitted pulse or the average power in the pulses.

## 6.6 Influence of pulse length

As discussed above, it is unfair to make any assessment of the contrast signal of the different measurements. Consequently no comparison in CTR and CNR will be done for the pulses of 2.5 and 3.5 periods. The TS can though be compared. As observed from figure 30 and 31, in AM both pulse lengths provide approximately the same level of suppression.<sup>3</sup> In PI and PIAM 2.5 period pulses offer 1.0 dB better TS compared to

---

<sup>1</sup>Be aware of that there is no big difference between PI full-band and filtered around 2<sup>nd</sup> harmonic, as PI has very little contrast signal on the fundamental.

<sup>2</sup>From the nonlinearity model in [12].

<sup>3</sup>The comparison is done with the AM filter applied.

3.5 period pulses. The suppression does thus seem to be superior for the shortest pulse when pulse inversion is applied, which might be due to asymmetry in the pulses not being corrected by the AM filter or more nonlinear response in tissue. But, of course, to conclude which pulse length is preferable the contrast signal must be evaluated too, which can not be done here. You should also be aware of the poorer radial resolution longer pulses bring along.

## 7 Suggested future work

From the discussion of the results a suggestion of a possible future modulation technique will be made. It is a three-pulse technique which employs a transmitted pulse packet of four pulses, where the first pulse is added to get rid of reverberations:

$$T_x = [0.5 \quad 0.5 \quad -1 \quad 0.5] \quad (34)$$

The echoes of the last three pulses are summed to create an image. This will first of all remove the linear signal. In addition will the reverberations from the pulses ahead of each imaging pulse sum to zero. Furthermore both the nonlinearities on the fundamental (from AM) and the *2nd* harmonic nonlinearities (mostly from PI) are present. And also phase shifts from the motion of the hart will be removed by summation, in the assumption of constant velocity. The drawback employing this technique is the reduced frame rate compared to a two-pulse PI technique.

Future experiments need to be performed to see if these assumed properties of the technique function as well as described above.

## 8 Conclusion

An investigation of pulses with different power, to be used in amplitude modulation, has shown a dissymmetry. As a result the method will suffer from a lower suppression of linear signal when a constant downscaling factor is employed in AM. To improve TS and CTR were filters tested out to replace the constant AM factor. Neither did the use of a filter based on electrical pulses nor a filter based on acoustical pulses outperform the constant AM factor. The filter from echo data gathered from a tissue phantom did however offer increased TS of 1.5-3.2 dB. The tissue filter does unfortunately also diminish the intensity of the contrast signal, but not as much as the increased TS, resulting in a gained CTR of 1.0-2.8 dB. As a consequence of the reduced contrast signal the CNR is lessened by a maximum of 0.6 dB.

Reverberations were dampened significantly by transmitting pulses in such a way that every pulse used to create an image has a relatively equal pulse in front. More exactly, the reverberation contributions from one pulse to the echoes of the next need to be summed to zero in the same manner as the linear tissue signal. Doing so, gives a TS enhancement of at least 13 dB in AM, compared to the results attained in the project work by the author [12].

Finally a suggestion of a three-pulse modulation technique was made. The packet consists of four pulses:  $[0.5 \ 0.5 \ -1 \ 0.5]$ , where the echoes of the last three are summed to create an image. This will remove both the linear signal and the reverberations. Furthermore the echoes from contrast bubbles will contain both pressure and phase dependent nonlinearities and phase shifts from hart movement will be eliminated.

## References

- [1] Angelsen B.A.J., Thorp H.G., *Ultrasound Imaging - Waves, Signals and Signal processing in Medical Ultrasonics*, Emantec, Norway, 2000. Chapter 1, 10 and 12.
- [2] Becher H., Burns P.N., *Handbook of Contrast Echocardiography*, Springer, 2000. Chapter 1
- [3] Eckersley R.J., Chin C.T., Burns P.N., *Optimising phase and amplitude modulation schemes for imaging microbubbles contrast agents at low acoustic power*, *Ultrasound in Med. and Bio.*, Vol. 31, No. 2 pp. 213-219, 2005.
- [4] Måsøy S.E., *Stochastic processes*, internal note NTNU, 2005.
- [5] Simpson D.H., *Detecting and imaging microbubble contrast agents with ultrasound*, Ph.D. thesis, University of Toronto, 2000. Chapter 1 and 2.
- [6] Kirkhorn J., 1999, *Introduction to IQ-demodulation of RF-data*, IFTB, NTNU, Sept. 15, 1999.
- [7] Van Trees H.L., *Detection, Estimation, and Modulation Theory*, John Wiley and Sons, Inc, 2001. Chapter 2.
- [8] Brock-Fisher G., Poland M., Rafter P. *Means for increasing sensitivity in nonlinear ultrasound imaging systems*. US patent 5577505, Nov. 26, 1996.
- [9] Phillips P.J., *Contrast pulse sequences (CPS): Imaging nonlinear microbubbles*. IEEE Ultrasonic Symposium 2001;2:1739-1745.
- [10] Wright J.N., *Image Formation in Diagnostic Ultrasound*. IEEE Ultrasonic Symposium 1997.
- [11] Jensen J.A., *Estimation of Blood Velocities using Ultrasound*, Cambridge University Press, UK, 1996.
- [12] Hofstad E.F., *In vitro resting og videreutvikling av deteksjonsmetoder for ultralyd kontrastmidler*, Project thesis, IFTB, NTNU, Norway, December 2005.
- [13] Frinking P.J.A., Bouakaz A., Kirkhorn J., Cate F.J.T., deJong N., *Ultrasound contrast imaging: Current and new potential methods*, *Ultrasound in Medicine and Biology*, 24(9):1419-1435, 1998.
- [14] Bjærum S., *Detection and Visualization of Moving Targets in Medical Ultrasound Imaging*, Norwegian University of Science and Technology, February 2001.
- [15] Steinsvik F., *Stepped Chirp - A new method for ultrasound contrast perfision imaging*.

*Simulations and in vitro experiments*, Diploma thesis, IFBT, NTNU, Norway, 2004.

## A Appendix

### A.1 Tissue Suppression

Table 8: *AM: Tissue Suppression [dB]*

	5/3.79V	7/5V	10/6.84V
2.5 p <sup>1</sup> , $\alpha^2$	28.0	29.6	30.4
2.5 p, H <sup>3</sup>	29.9	32.8	32.8
3.5 p, $\alpha$	28.4	30.3	30.6
3.5 p, H	30.3	32.5	32.1

Table 9: *PIAM: Tissue Suppression [dB]*

	5/3.79V	7/5V	10/6.84V
2.5 p, $\alpha$	25.1	24.4	21.8
2.5 p, H	26.6	25.8	24.4
3.5 p, $\alpha$	24.7	23.8	20.7
3.5 p, H	26.0	24.5	23.3

Table 10: *PI: Tissue Suppression [dB]*

	5/3.79V	7/5V	6.08/4.45V	10/6.84V
2.5 p	23.9	22.5	21.4	16.7
3.5 p	23.3	21.5	20.3	15.3

<sup>1</sup>p: Number of periods in transmitted pulses.

<sup>2</sup> $\alpha$ : A constant downscaling factor is use in AM and PIAM.

<sup>3</sup>H: A filter is use instead of  $\alpha$  in AM and PIAM.



## A.2 Contrast-to-Tissue-Ratio

Table 11: AM: Contrast-to-Tissue-Ratio [dB]

	5/3.79V	7/5V	10/6.84V
2.5 p, Optison, $\alpha$	16.3	16.3	15.0
2.5 p, Optison, H	17.3	19.1	17.1
3.5 p, Optison, $\alpha$	19.4	18.6	18.8
3.5 p, Optison, H	20.7	20.0	20.3
2.5 p, Sonazoid, $\alpha$	17.6	14.7	15.0
2.5 p, Sonazoid, H	18.8	15.8	17.1
3.5 p, Sonazoid, $\alpha$	16.6	20.9	20.1
3.5 p, Sonazoid, H	17.9	22.1	21.9

Table 12: PIAM: Contrast-to-Tissue-Ratio [dB]

	5/3.79V	7/5V	10/6.84V
2.5 p, Optison, $\alpha$	18.3	13.5	8.8
2.5 p, Optison, H	18.9	14.4	10.3
3.5 p, Optison, $\alpha$	20.7	16.1	14.4
3.5 p, Optison, H	21.0	17.3	15.7
2.5 p, Sonazoid, $\alpha$	19.0	12.9	8.6
2.5 p, Sonazoid, H	19.8	13.9	9.6
3.5 p, Sonazoid, $\alpha$	17.8	17.3	14.2
2.5 p, Sonazoid, H	19.1	18.6	15.9

Table 13: *PI: Contrast-to-Tissue-Ratio [dB]*

	5/3.79V	7/5V	6.08/4.45V	10/6.84V
2.5 p, Optison	22.0	19.0	15.1	8.9
3.5 p, Optison	24.2	19.7	16.1	13.0
2.5 p, Sonazoid	21.6	17.2	13.4	7.6
3.5 p, Sonazoid	20.4	18.0	17.3	13.0

### A.3 Contrast-to-Noise-Ratio

Table 14: *AM: Contrast-to-Noise-Ratio [dB]*

	5/3.79V	7/5V	10/6.84V
2.5 p, Optison, $\alpha$	20.2	22.8	25.2
2.5 p, Optison, H	19.9	22.5	25.2
3.5 p, Optison, $\alpha$	23.2	24.9	28.7
3.5 p, Optison, H	22.8	23.5	28.2
2.5 p, Sonazoid, $\alpha$	21.6	21.4	24.6
2.5 p, Sonazoid, H	21.3	21.2	24.6
3.5 p, Sonazoid, $\alpha$	20.6	27.1	30.0
3.5 p, Sonazoid, H	20.4	26.1	29.8

Table 15: *PIAM: Contrast-to-Noise-Ratio [dB]*

	5/3.79V	7/5V	10/6.84V
2.5 p, Optison, $\alpha$	24.3	24.9	26.5
2.5 p, Optison, H	23.8	24.7	25.8
3.5 p, Optison, $\alpha$	27.6	28.5	33.8
3.5 p, Optison, H	26.6	26.7	32.4
2.5 p, Sonazoid, $\alpha$	25.6	24.3	26.7
2.5 p, Sonazoid, H	25.0	24.1	26.5
3.5 p, Sonazoid, $\alpha$	25.0	29.9	34.1
3.5 p, Sonazoid, H	24.0	29.1	33.6

Table 16: *PI: Contrast-to-Noise-Ratio [dB]*

	5/3.79V	7/5V	6.08/4.45V	10/6.84V
2.5 p, Optison	27.8	29.0	27.9	30.2
3.5 p, Optison	31.2	31.2	30.7	36.5
2.5 p, Sonazoid	28.2	27.8	26.7	29.6
3.5 p, Sonazoid	27.7	29.8	32.2	37.0